Research article

JHEP|Reports

Loss of *Cdkn1a* protects against MASLD alone or with alcohol intake by preserving lipid homeostasis

Authors

Arantza Lamas-Paz, Alejandro Hionides-Gutiérrez, Feifei Guo, …, Pere Puigserver, Yulia A. Nevzorova, Francisco Javier Cubero

Correspondence

fcubero@ucm.es (F.J. Cubero).

Graphical abstract

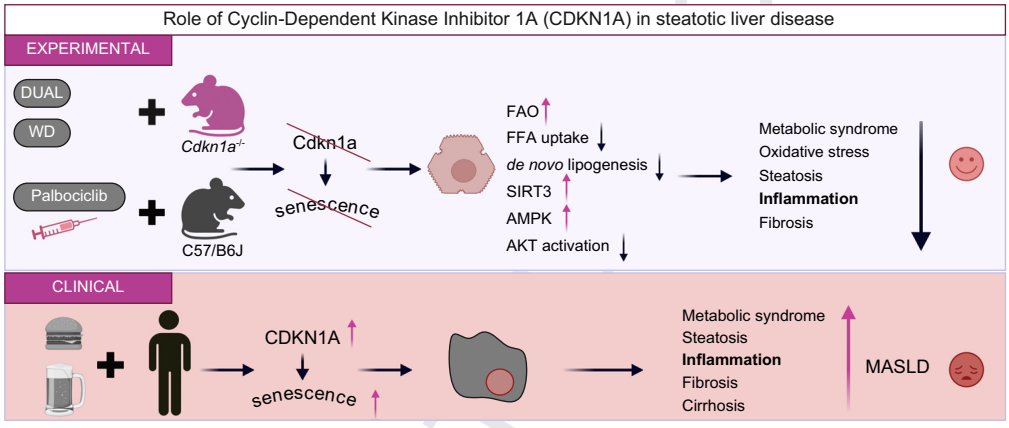

Highlights:

- CDKN1A contributes to the stability of cell cycle arrest after the induction of senescence.
- Liver senescence is responsible for the metabolic shifts causing fat accumulation and hepatic inflammation in patients with SLD.
- Loss of *Cdkn1a* has a protective effect in preclinical metabolically induced SLD, with and without alcohol consumption.
- *CDKN1A* expression correlates with NAFLD activity score and advanced fibrosis in patients with MASLD.

Impact and implications:

Expression of p21, encoded by the *CDKN1A* gene, has been associated with fibrosis progression in steatotic liver disease (SLD), but the molecular mechanisms remain elusive. Interestingly, in this study we found that *Cdkn1a* deletion protected against preclinical SLD by promoting fatty acid oxidation and preventing free fatty acid uptake and *de novo* lipogenesis, via the AMPK-SIRT3 axis. Translationally, *Cdkn1a* expression was found to be directly correlated with increased severity of NAFLD Activity Score (NAS) and fibrosis in SLD patients, and therefore, CDKN1A might be used potential theragnostic target for the treatment of metabolically induced SLD, with and without alcohol consumption.

https://doi.org/10.1016/j.jhepr.2024.101230

Research article

JHEP|Reports

Loss of *Cdkn1a* protects against MASLD alone or with alcohol intake by preserving lipid homeostasis

Arantza Lamas-Paz[1,2,†], **Alejandro Hionides-Gutiérrez**[1,†], **Feifei Guo**[1,3,†], Gonzalo Jorquera[4,5], Laura Morán-Blanco[1], Raquel Benedé-Ubieto[1], Mariana Mesquita[1,6], Olga Estévez-Vázquez[1], Kang Zheng[1,7], Marina Mazariegos[1], Elena Vázquez-Ogando[8,9,10], Elena Blázquez-López[8,9,10], Iris Asensio[8,9,10], Beste Mutlu[11,12], Beatriz Gomez-Santos[13,14], María Isabel Peligros[15], Javier Vaquero[8,9,10], Rafael Bañares[8,9,10], Teresa C. Delgado[16], María Luz Martínez-Chantar[10,16], Eduardo Martínez-Naves[1,2], Carlos Sanz-García[1], Mohamed Ramadan Mohamed[17], Sofía Tesolato[18,19], Pilar Iniesta[18,19], Rocío Gallego-Durán[10,20], Douglas Maya-Miles[10,20], Javier Ampuero[10,20], Manuel Romero-Gómez[10,20], Ana Martínez-Alcocer[10,21], David Sanfeliu-Redondo[10,21], Anabel Fernández-Iglesias[10,21], Jordi Gracia-Sancho[10,21,22], Mar Coll[10,23], Isabel Graupera[10,23,24], Pere Ginès[10,23,24], Andrea Ciudin[25,26], Jesús Rivera-Esteban[27,28], Juan M. Pericàs[10,27], Matías A. Ávila[10,29,30], Maria Dolores Frutos[31], Carlos Manuel Martínez-Cáceres[32], Bruno Ramos-Molina[33], Patricia Aspichueta[10,13,14], Pere Puigserver[11,12,‡], Yulia A. Nevzorova[1,9,10,‡], Francisco Javier Cubero[1,9,10,*,‡]

JHEP Reports **2025**. vol. 7 | 1–15

Background & Aims: Expression of P21, encoded by the *CDKN1A* gene, has been associated with fibrosis progression in steatotic liver disease (SLD); however, the underlying mechanisms remain unknown. In the present study, we investigated the function of CDKN1A in SLD.

Methods: *CDKN1A* expression levels were evaluated in different patient cohorts with SLD, fibrosis, and advanced chronic liver disease (ACLD). *Cdkn1a*$^{-/-}$ and *Cdkn1a*$^{+/+}$ mice were fed with either a Western diet (WD), a Lieber-DeCarli (LdC) diet plus multiple EtOH (ethanol) binges, or a DuAL diet (metabolic dysfunction-associated fatty liver disease and alcohol-related liver). Primary hepatocytes were isolated and functional assays performed.

Results: A significant increase in *CDKN1A* expression was observed in patients with steatohepatitis and fibrosis (with a positive correlation with both NAFLD Activity Score and fibrosis staging scores), cirrhosis and ACLD. *Cdkn1a*$^{+/+}$ mice, fed a DuAL diet exhibited liver injury and cell death increased reactive oxygen species (ROS), and markers of senescence (γH2AX, β-GAL, *Cdkn1a*/*p53*) contributing to steatosis and inflammation. In contrast, *Cdkn1a*$^{-/-}$ mutant mice showed a significant decrease in senescence-associated markers as well as in markers of liver injury, hepatic steatosis and an increase in fatty acid oxidation and reduction in free fatty acid uptake as well as *de novo* lipogenesis. Mechanistically, activation of the AMPK-SIRT3 was observed in *Cdkn1a*-deleted animals.

Conclusions: *Cdkn1a* deletion protected against preclinical SLD by promoting fatty acid oxidation and preventing free fatty acid uptake and *de novo* lipogenesis via the AMPK-SIRT3 axis. *CDKN1A* expression was found to be directly correlated with increased severity of NAFLD Activity Score and fibrosis in patients with SLD. CDKN1A could be a potential theragnostic target for the treatment of metabolic dysregulation in patients with SLD, with and without alcohol consumption.

Introduction

Cyclin-dependent kinase inhibitor 1A (CDKN1A) is a member of the cyclin-dependent kinases inhibitors (CDKN) of the Cip/Kip family[1] that arrests cells by affecting the activity of cyclin D-, E-, and A-dependent kinases, which regulate progression through the G1 phase of the cell cycle and inhibition of DNA synthesis.[2] CDKN1A also inhibits proliferation competing with proliferating cell nuclear antigen (PCNA)[3] or indirectly at the transcriptional level.[4] CDKN1A contributes to the stability of cell cycle arrest long after the induction of senescence.[5] Microarray-based studies suggested that CDKN1A expression positively correlates with both the suppression of genes involved in cell cycle progression, and the induction of senescence genes.[5]

Cellular senescence develops in response to cellular injury, leading not only to cell cycle arrest, but also to alterations of the cellular phenotype and metabolic functions.[6] A plethora of evidence suggested that liver senescence, and particularly hepatocytic senescence, is responsible for the metabolic shifts causing fat accumulation and liver inflammation in patients with steatotic liver disease (SLD), the main overarching cause of chronic liver disease (CLD).[7]

* Corresponding author. Address: Department of Immunology, Ophthalmology and ENT, Complutense University School of Medicine, c/Doctor Severo Ochoa, 9, 28040, Madrid, Spain. Tel.: +34 91394 1385.
E-mail address: fcubero@ucm.es (F.J. Cubero).
† Authors contributed equally as first authors.
‡ Authors contributed equally as senior authors.
https://doi.org/10.1016/j.jhepr.2024.101230

CLD represents a major health problem, representing the 10th cause of death worldwide, with 2 million individuals dying of liver disease each year.[8] CLD is defined as the progressive deterioration of liver functions with a continuous process of inflammation, destruction, and regeneration of liver parenchyma, which leads to fibrosis and cirrhosis.[9] The spectrum of etiologies is broad for CLD, including SLD with or without potentially harmful alcohol intake, the latter known as MetALD.[10] Metabolic dysfunction-associated SLD (MASLD), its more rapidly growing form, ranges from steatosis to steatohepatitis and cirrhosis. Moreover, metabolic dysfunction can synergize with harmful alcohol consumption (MetALD), which can induce SLD (alcohol-related liver disease [ALD]). Both MASLD and MetALD are hepatic insults that range from simple steatosis to advanced CLD, including cirrhosis and hepatocellular carcinoma (HCC).[11]

Several studies showed an association between CDKN1A expression and the progression of CLD.[12–16] Increased CDKN1A expression is evidenced in animal models of obesity[14,17] and in patients with SLD.[15] Therefore, we sought to investigate whether the development of SLD and its progression to steatohepatitis, commonly accompanied by several pathophysiological events including metabolic dysregulation and inflammatory phenomena occurring within the liver, may derive from CDKN1A-derived induction of cellular senescence, triggering metabolic alterations. Moreover, we explored the pharmacological inhibition of CDKN1A in preclinical SLD using palbociclib.

Altogether, our data strongly support the notion that CDKN1A has a protective effect against preclinical metabolically induced SLD, with and without alcohol consumption, and might be an optimal theragnostic tool for the progression of CLD.

Materials and methods

Patient cohorts

This multicentric study was composed of several cohorts. Cohort #1 is a metanalysis (Table S1) that integrated data from three different studies, mostly patients with MASLD, with different stages of fibrosis (F0–F4), in which expression of *CDKN1A* was analyzed using RNAseq. All data were integrated into a single analysis in which each study was treated as a batch.

Cohort #2 consisted of 91 consecutive and prospective individuals recruited for a bariatric intervention in the Virgen de la Arrixaca University Hospital (Murcia, Spain), with suspicion of MASLD.[18] The study was approved by the Ethics and Clinical Research Committees of the Virgen de la Arrixaca University Hospital (ref. number 2020-2-4-HCUVA). A recently characterized cohort (cohort #3) (22 patients)[19] encompassing the whole spectrum of CLD stages to any cause of SLD, ranging from patients with early fibrosis to compensated cirrhosis (CC) was also used. F1/F2/F3 fibrosis, named early-CLD to CC was also used. The protocol of the study was approved by the Institutional Review Board of the Hospital Clinic of Barcelona (code: 2012/7977).

Cohort #4 consisted of 13 patients from a previously published study[20] with advanced CLD (decompensated cirrhosis) that underwent liver transplantation and control patients with no suspected CLD, who underwent liver resection as a result of colorectal carcinoma metastasis. The study's first stage, in which the miRNA signature was identified, was conducted at the August Pi i Sunyer Biomedical Research Institute-Hospital Clinic of Barcelona, and its protocol was approved by this center's Ethics Committee (HCB/2018/0028). The protocol for subsequent stages received approval from the Ethics Committee for Clinical Research of the Hospital Universitario Ramon y Cajal (institutional review board number 362/19; approval date April 1, 2019). All included individuals provided written informed consent authorizing the storage and research use of their biological samples.

Animal experimentation

Eight-to 13-week-old male *Cdkn1a*$^{-/-}$ knockout mice (B6;129S2 Cdkn1atm1Tyj/J, The Jackson Laboratory, Bar Harbor, ME, USA) and *Cdkn1a*$^{+/+}$ mice (B6;129SF2/J, The Jackson Laboratory) were maintained in the animal Facility of the Faculty of Biology at Complutense University of Madrid (UCM), in a temperature- and humidity-controlled room with a 12-h light/dark cycle and allowed food and water *ad libitum,* according to the guidelines of the Federation for Laboratory Animal Science Associations (FELASA). All animal procedures were carried out according to Spanish legal requirements and animal protection law and approved by the authority of environment conservation and consumer protection of the Regional Government of Madrid (PROEX-397.2/21).

Cdkn1a$^{-/-}$ and *Cdkn1a*$^{+/+}$ mice were fed with a DuAL diet (metabolic dysfunction-associated fatty liver disease and alcohol-related liver; n = 6–10) consisting of Western diet (WD) (D18121807, Research Diets, Inc., New Brunswick, NJ, USA) and 10% vol/vol absolute ethanol (EtOH) in drinking sweetened water (6.75% D-glucose, Merck, Madrid, Spain) for 18 weeks[21]; a WD (D18121807, Research Diets, Inc.) (n = 8–12) for 14 weeks and an EtOH diet (n = 7–13) where mice were allowed free access to 5.07% w/v (6.4% v/v) EtOH Lieber-DeCarli (LdC) liquid diet (F1258SP, Bio-Serv, Madrid, Spain) for 8 weeks plus a 30% EtOH gavage (6 g/kg body weight [BW]) every 2 weeks.[22] C57BL/6 WT mice were also fed with DuAL diet for 10 weeks, plus an administration of 100 mg/kg of palbociclib (MedChemExpress, Madrid, Spain) via oral gavage twice a week. Controls were fed with normal chow diet (Altomin, Lage, Germany) and filtered tap water or LdC control diet, where the remainder of the energy is provided as carbohydrates, which in the EtOH formula was isocalorically replaced by EtOH.

At the end of each experiment, all animals were fasted overnight for 12 h and sacrificed by an overdose of isoflurane (Solvet, Segovia, Spain) and liver and blood were collected.

Statistical analysis

Data are expressed as mean ± SD. GraphPad Prism version 8.0 (GraphPad Software Inc., San Diego, CA, USA) was used to perform statistical analysis. Data are expressed as mean ± SD. For each experiment, statistical details can be found in the figure legends, including statistical tests and sample sizes. To evaluate the statistical differences between *Cdkn1a*$^{-/-}$ and *Cdkn1a*$^{+/+}$ mice and *siCtrl* and *siCdkn1a* primary hepatocytes in functional assays ANOVA one-way Tukey *post hoc* test was used. Additionally, statistical significance between *siCtrl* and *siCdkn1a* primary hepatocytes in quantitative PCR (qPCR) assays was determined using Student *t* test. In general, a

value of p <0.05 was considered significant. Pearson correlation was utilized to assess the relationship between gene expressions.

Results

Expression of CDKN1A and SASP in patients with MASLD/MASH and fibrosis

Significantly increased gene counts for *CDKN1A* were observed in a RNAseq dataset of patients with diagnosed MASLD with NAFLD Activity Score (NAS) >4 (Fig. 1A, cohort #1). Thus, we next analyzed CDKN1A protein expression in liver extracts of patients with MASLD. Interestingly, we observed progressive overexpression of CDKN1A in patients with high NAS score (Fig. S1A, cohort #2).

Considering that hepatic fibrosis is an important factor affecting the prognosis of liver diseases, we next evaluated whether CDKN1A was also significantly upregulated in cohorts of patients with fibrosis. CDKN1A gene counts significantly increased from F1 to F4 (Fig. S1B, cohort #1), and, especially, between F0–F2 and F3–F4 (Fig. 1B, cohort #1). Liver fibrosis involves cell cycle re-entry and proliferation of parenchymal and non-parenchymal liver cells controlled by cyclins and associated cyclin-dependent kinases (CDKs). Hence, all cyclins and CDKs tested in cohort #1 were significantly downregulated in F0–F2 compared with F3–F4 (Fig. S1C), indicating the importance of cell cycle in hepatic fibrogenesis. Of note, the area under the receiver operating characteristic curve (AUROC) when assessing CDKN1A was 0.81 (95% CI 0.72–0.89) for fibrosis prediction (Fig. 1C).

To validate the utility of CDKN1A in patients with MASLD patients, we examined the correlation of CDKN1A with the NAS and the fibrosis score. CDKN1A positively correlated with NAS (Fig. 1D, Fig. S1D, cohort #1) and the fibrosis score (Fig. 1E, Fig. S1E, cohort #1), highlighting the prognostic value of this gene in MASLD and fibrosis.

Moreover, increased mRNA expression of *CDKN1A* was observed in patients with early CLD with F2/F3 fibrosis score

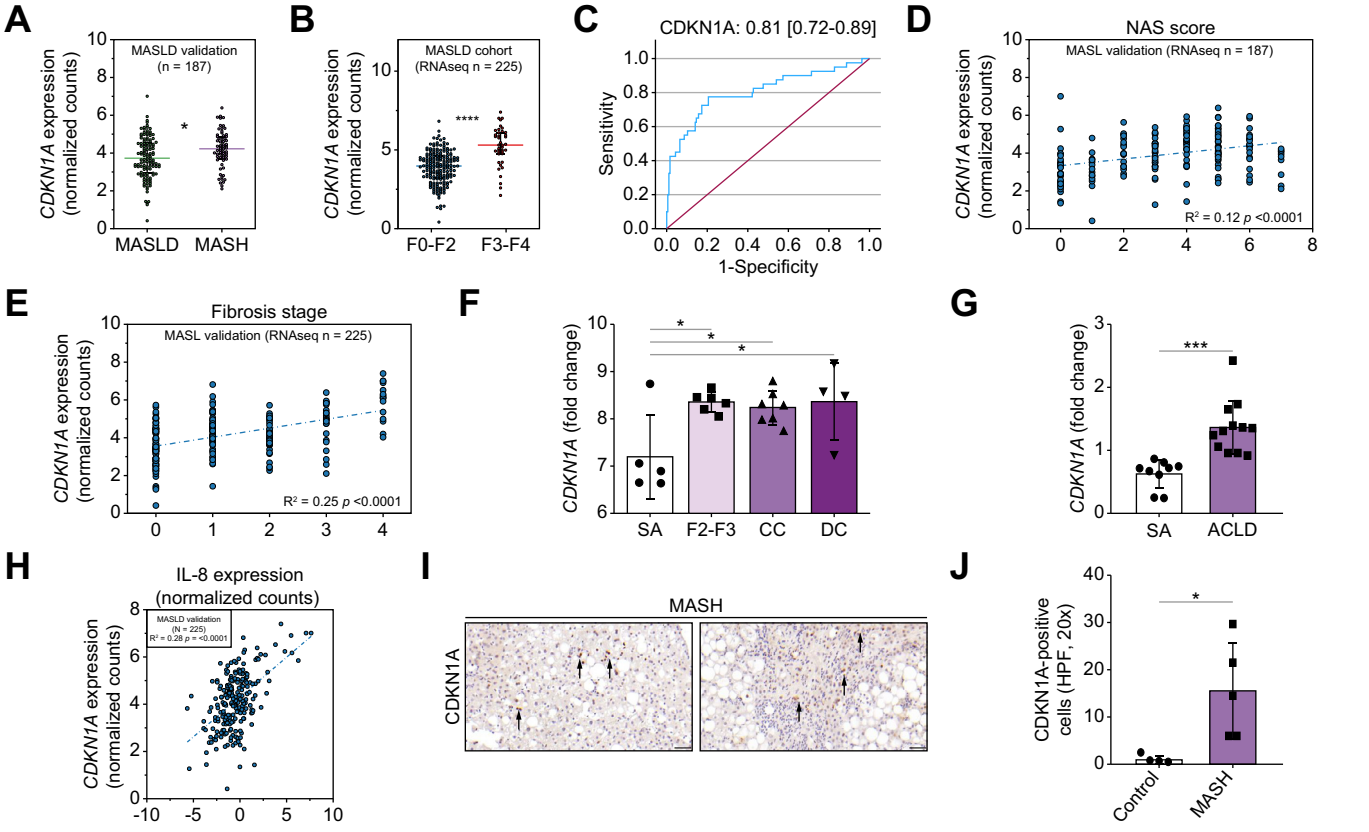

Fig. 1. CDKN1A expression is characteristic of patients with SLD and fibrosis. (A) Cohort #1. *CDKN1A* mRNA relative expression to GAPDH in livers of patients with MASLD and MASH, identified with a NAS score ≥5 (n = 187). (B) Cohort #1. *CDKN1A* mRNA relative expression to GAPDH in livers of patients with MASLD with a fibrosis score between F0–F2 and F3–F4 (n = 225). (C) Cohort #1. AUROC when assessing CDKN1A for fibrosis prediction. AUROC of 0.81 (95% CI 0.72–0.89) for fibrosis prediction. (D) Cohort #1. Correlation between *CDKN1A* mRNA relative expression to GAPDH in livers of patients with MASLD with a NAS score >4 (n = 187). (E) Cohort #1. Correlation between *CDKN1A* mRNA relative expression to *GAPDH* in livers of patients with MASLD with a fibrosis score F0–F2 and F3–F4 (n = 225). (F) Cohort #3. *CDKN1A* mRNA relative expression to GAPDH in livers of non-affected patients and patients with a fibrosis score between F2 and F4 and compensated cirrhosis (CC) and decompensated cirrhosis (DC) (n = 22). (G) Cohort #4. *CDKN1A* mRNA relative expression to GAPDH in livers of patients with ACLD and non-affected patients (n = 13). (H) Cohort #1. Correlation between *IL-8* mRNA relative expression to GAPDH in livers of patients with MASLD. (I) Immunostaining for CDKN1A was tested in paraffin sections of patients with a diagnosis of MASH with the presence of steatosis and inflammation. Microphotographs were taken at 300 μm. (J) Quantification of positive cells was performed and graphed, 200 hepatocytes per field were counted. Student *t* test was performed (*p <0.05; ****p <0.0001). ACLD, advanced chronic liver disease; AUROC, area under the receiver operating characteristic curve; CDKN1A, cyclin-dependent kinase inhibitor 1A; GADPH, glyceraldehyde-3-phosphate dehydrogenase; MASLD, metabolic dysfunction-associated steatotic liver disease; MASH, metabolic-associated steatohepatitis; NAS, NAFLD Activity Score; SLD, steatotic liver disease.

(Fig. 1F, cohort #3), CC and decompensated cirrhosis (DC), and with advanced CLD (Fig. 1G, cohort #4).

Inflammation is a significant component of MASLD and is closely linked to the senescence-associated secretory phenotype (SASP). Therefore, we analyzed the correlation between the levels of proinflammatory cytokines in patients with MASLD. Interestingly, we found a significant correlation of *IL8* (Fig. 1H, cohort #1), and *IL6ST* with patients with MASLD (Fig. S1F, cohort #1). Finally, to understand hepatocytic or non-parenchymal cells (NPC)-associated expression of CDKN1A/P21, we performed immunohistochemical (IHC) staining in paraffin sections of patients diagnosed with MASLD/metabolic-associated steatohepatitis (MASH). Interestingly, CDKN1A expression was restricted to hepatocyte nuclei and characteristic of patients with MASLD/MASH compared with non-affected tissue (normal) (Fig. 1I,J, Fig. S1G, cohort #2).

Loss of *Cdkn1a* protects mice from liver injury after a DuAL diet

To understand the theragnostic value of CDKN1A in the progression of liver disease, we first analyzed the mRNA expression of *Cdkn1a* in isolated liver cells. Interestingly, *Cdkn1a* expression was highly expressed in hepatocytes, but also in NPCs-hepatic stellate cells (HSCs) and Kupffer cells (KCs) (Fig. S2A). We subsequently evaluated *Cdkn1a* expression in preclinical models of MASLD/MetALD. *Cdkn1a* mRNA expression was significantly upregulated in wildtype mice after DuAL and WD diet compared with chow-fed animals, whereas no differences were observed in the EtOH-fed group (Fig. S2B). At the protein level, overexpression of CDKN1A was characteristic of mice fed a DuAL diet (Fig. S2C). These results indicated that CDKN1A might play an important role in preclinical MASLD with alcohol intake.

Therefore, we subsequently focused on examining the role of CDKN1A in the DuAL model, which mimics the clinical features of MASLD and chronic moderate harmful alcohol consumption during 18 weeks of treatment. *Cdkn1a*$^{+/+}$ animals fed a DuAL diet exhibited enlarged livers and significantly elevated liver weight (LW) and LW/body weight (BW) ratio, albeit no differences in BW (Fig. 2A, Fig. S3A–C). However, this increase was significantly reduced in *Cdkn1a*$^{-/-}$ compared with *Cdkn1a*$^{+/+}$ mice (Fig. 2A, Fig. S3A–C). Concomitantly, serum markers of liver damage including alanine aminotransferase (ALT) (Fig. 2B), aspartate aminotransferase (AST) and lactate dehydrogenase (Figs. S3D and E) were significantly decreased in *Cdkn1a*$^{-/-}$ compared with *Cdkn1a*$^{+/+}$ mice fed a DuAL diet.

Histopathologically, *Cdkn1a*$^{+/+}$ livers displayed hepatocyte enlargement, ballooning, steatosis, and cell death (Fig. 2C, Fig. S3F). DuAL-fed mice exhibited the first signs of fibrosis as soon as 10 weeks of injury with remarkable escalation of fibrogenesis at 23 weeks.[21] These findings were additionally confirmed in *Cdkn1a*$^{+/+}$ mice, fed a DuAL diet for 18 weeks, as observed by significantly increased *αSma* and *CollagenIA1* mRNA expression, Sirius Red and Vimentin IHC stainings (Fig. 2D–F, Fig. S3G,H, Fig. S4A,B). However, these parameters were significantly decreased in *Cdkn1a*$^{-/-}$ animals (Fig. 2D–F, Fig. S3G,H, Fig. S4A,B).

As liver fibrosis is a common feature of chronic liver injury and is initiated by cell death inside the liver, we next studied the levels of proteins related to liver cell death. Interestingly, cleaved caspase-3 (CC3) and -8 (CC8), pRIPK1/3, and pMLKL were significantly overexpressed in *Cdkn1a*$^{+/+}$, compared with *Cdkn1a*$^{-/-}$ mice fed a DuAL diet (Fig. 2G). Consistently, cell death, measured by terminal deoxynucleotidyl transferase-mediated deoxyuridine triphosphate nick-end labeling (TUNEL) staining, was also significantly higher in *Cdkn1a*$^{+/+}$ animals, whereas it was significantly decreased in *Cdkn1a*$^{-/-}$ mice fed a DuAL diet (Fig. 2H).

Because of the role of CDKN1A in the progression of cell cycle in the G1 phase as an inhibitor,[12] we evaluated the mRNA transcripts of cell cycle mediators controlling the late G1-and S-phase progression. Therefore, we measured the number of transcripts of cyclins including *CcnA2, D1*, and *E1* (Fig. 2I–K). Interestingly, the levels of *CcnA2*, *D1* transcripts were significantly decreased in *Cdkn1a*$^{-/-}$ animals, whereas no differences were found in *CcnE1* mRNA expression between *Cdkn1a*$^{+/+}$ and *Cdkn1a*$^{-/-}$ (Fig. 2I–K). Furthermore, no statistical significance was observed in Ki67-positive cells in *Cdkn1a*$^{-/-}$, compared with *Cdkn1a*$^{+/+}$ animals fed a DuAL diet (Figs. S4C and D).

Deletion of *Cdkn1a* protects against preclinical SLD

As the DuAL preclinical model represents the combined synergistic effect of both a WD and harmful alcohol intake, we next examined the role of CDKN1A in each of the factors alone. Therefore, WD treatment was performed over 14 weeks in *Cdkn1a*$^{+/+}$ and *Cdkn1a*$^{-/-}$ mice (Fig. 3). Interestingly, a significant decrease in the LW/BW ratio (Fig. 3A, Fig. S5A), as well as in serum markers of liver damage – ALT (Fig. 3B) and AST (Fig. S5B) were observed in *Cdkn1a*$^{-/-}$ mice fed a WD. The histopathological study of liver sections by H&E showed macrosteatosis mainly surrounding the portal spaces and predominant microsteatosis located in the perivenular areas of *Cdkn1a*$^{+/+}$ animals, fed a WD (Fig. 3C, Fig. S5C). However, liver architecture was preserved in *Cdkn1a*$^{-/-}$ mice.

Moderately enhanced chicken wire fibrosis appeared along with sinusoidal and periportal fibrillar collagen deposition in both *Cdkn1a*$^{+/+}$ and *Cdkn1a*$^{-/-}$ mice fed a WD diet (Fig. 3D,F, Fig. S5D). Apart from this mild fibrosis, the WD triggered cell death in the hepatic parenchyma, analyzed as TUNEL-positive cells in *Cdkn1a*$^{+/+}$. Interestingly, mice with deletion of *Cdkn1a* displayed significantly decreased TUNEL positivity (Fig. 3E,G, Fig. S5E), albeit no differences in cell proliferation (Fig. 5F,G).

Furthermore, we assessed insulin resistance using the glucose tolerance test (GTT) in mice after WD feeding. GTT results and basal glucose levels measured in blood in *Cdkn1a*$^{+/+}$ animals showed a delay in glucose uptake after WD; however, not significant compared to *Cdkn1a*$^{-/-}$ mice (Fig. S6A). The area under the curve of the GTT test exhibited a statistically significance disparity only between the chow and WD-fed *Cdkn1a*$^{-/-}$ mice. However, no statistical significance was observed in *Cdkn1a*$^{+/+}$ mice when compared with *Cdkn1a*$^{-/-}$ mice (Fig. S6B). Of note, basal levels of glucose in blood were significantly lower in *Cdkn1a*$^{-/-}$ mice after a chow diet (Fig. S6C), indicating that metabolism might be dysregulated in this mouse strain.

Altogether, these results suggest that *Cdkn1a* deletion protects against a preclinical model of SLD.

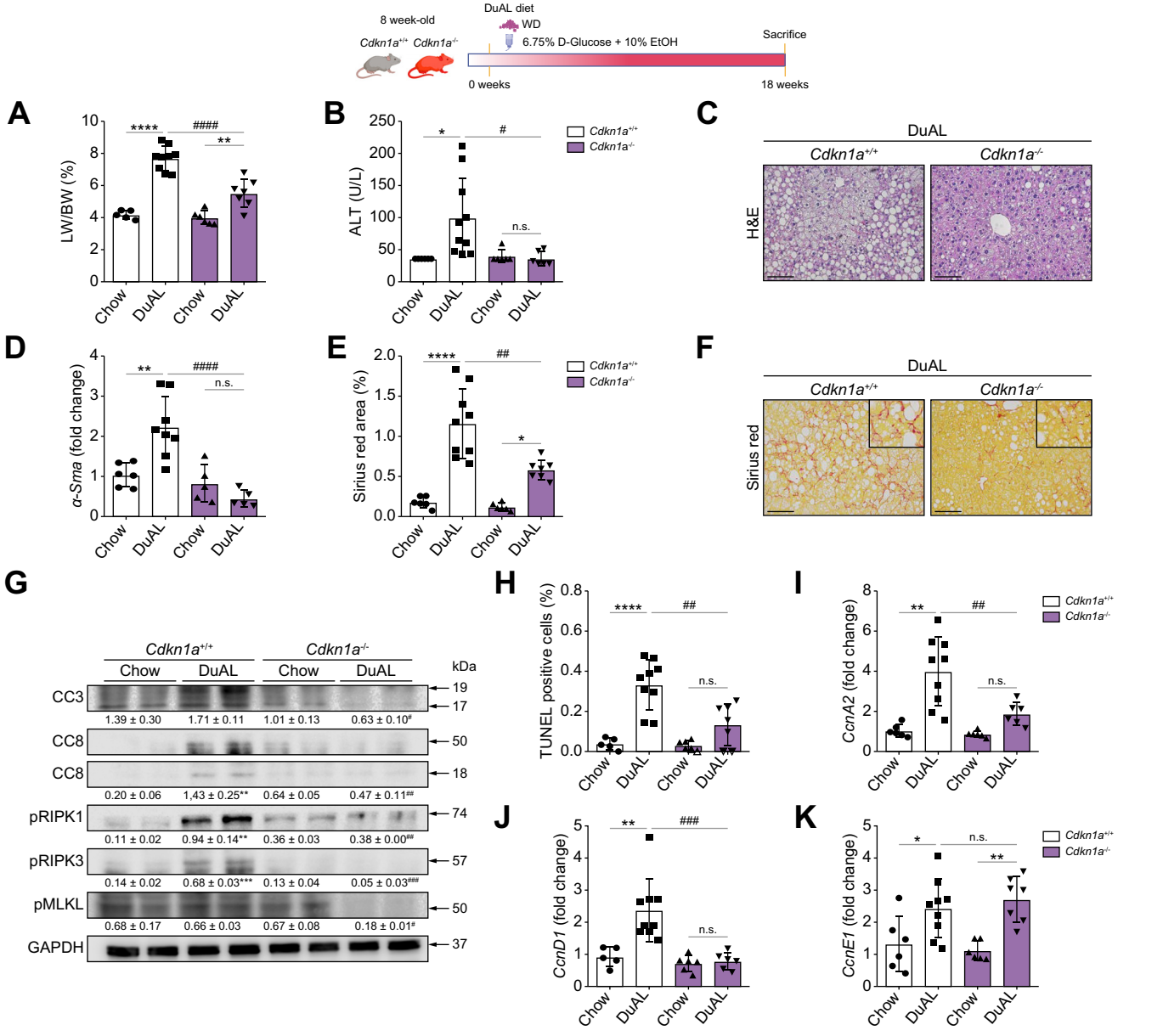

Fig. 2. Liver injury is significantly reduced after a DuAL diet in *Cdkn1a*$^{-/-}$ mice. Schematic description of a DuAL model performed in *Cdkn1a*$^{+/+}$ and *Cdkn1a*$^{-/-}$ mice. (A) Liver weight to body weight ratio (%). (B) Serum ALT levels. (C) H&E staining in *Cdkn1a*$^{+/+}$ and *Cdkn1a*$^{-/-}$ mice after DuAL diet. Scale bar = 100 μm. (D) α-*Sma* mRNA relative liver expression to *Gapdh*. (E) Sirius red staining quantification in *Cdkn1a*$^{+/+}$ and *Cdkn1a*$^{-/-}$ mice after DuAL diet and (F) representative paraffin liver sections stained. Scale bar = 100 μm. (G) Total liver protein (two individuals' samples from each group are shown as representative of the group) were isolated from DuAL diet-fed *Cdkn1a*$^{+/+}$ and *Cdkn1a*$^{-/-}$ mice and analyzed for CC-3, CC-8, pRIPK1, pRIPK3, and pMLKL. Protein expression levels were normalized to the levels of total GAPDH and the ratio was calculated. (H) Quantification of TUNEL-positive cells (%) was done and graphed. (I) *CcnA2*, (J) *CcnD1*, and (K) *CcnE1* measured in mice of each group relative to *Gapdh*. Scale bar = 100 μm. n = 6–10; one-way ANOVA with *post hoc* Tukey test was used for the calculations (intragroup: **p* <0.05, *****p* <0.0001; intergroup: #*p* <0.05, ####*p* <0.0001). ALT, alanine aminotransferase; BW, body weight; CC3, cleaved-caspase-3; CC8, cleaved-caspase-8; *CcnA2*, ciclyn A2; *CcnD1*, cyclin D1; *CcnE1*, ciclin E1; *Cdkn1a*, cyclin-dependent kinase inhibitor 1A; DuAL, metabolic dysfunction-associated fatty liver disease and alcohol-related liver; GADPH, glyceraldehyde-3-phosphate dehydrogenase; LW, liver weight; RIPK, receptor interacting protein kinase; TUNEL, terminal deoxynucleotidyl transferase-mediated deoxyuridine triphosphate nick-end labeling.

CDKN1A knockout mice are not protected against murine ALD

To further explore the relevance of CDKN1A in preclinical ALD, we performed an acute-on-chronic LdC diet plus multiple EtOH binges, a modification of the National Institute on Alcohol Abuse and Alcoholism model,[22] in *Cdkn1a*$^{+/+}$ and *Cdkn1a*$^{-/-}$ mice. No differences were observed macroscopically in livers or in the LW/BW ratio between *Cdkn1a*$^{+/+}$ and *Cdkn1a*$^{-/-}$ animals (Fig. 3H, Fig. S7A). Accordingly, serum markers of liver damage (ALT, AST) were elevated in both *Cdkn1a*$^{+/+}$, and *Cdkn1a*$^{-/-}$ fed a LdC, compared with control diet-fed mice (Fig. 3I, Fig. S7B). Alcohol metabolism by CYP2E1 (cytochrome P450) levels showed a similar induction

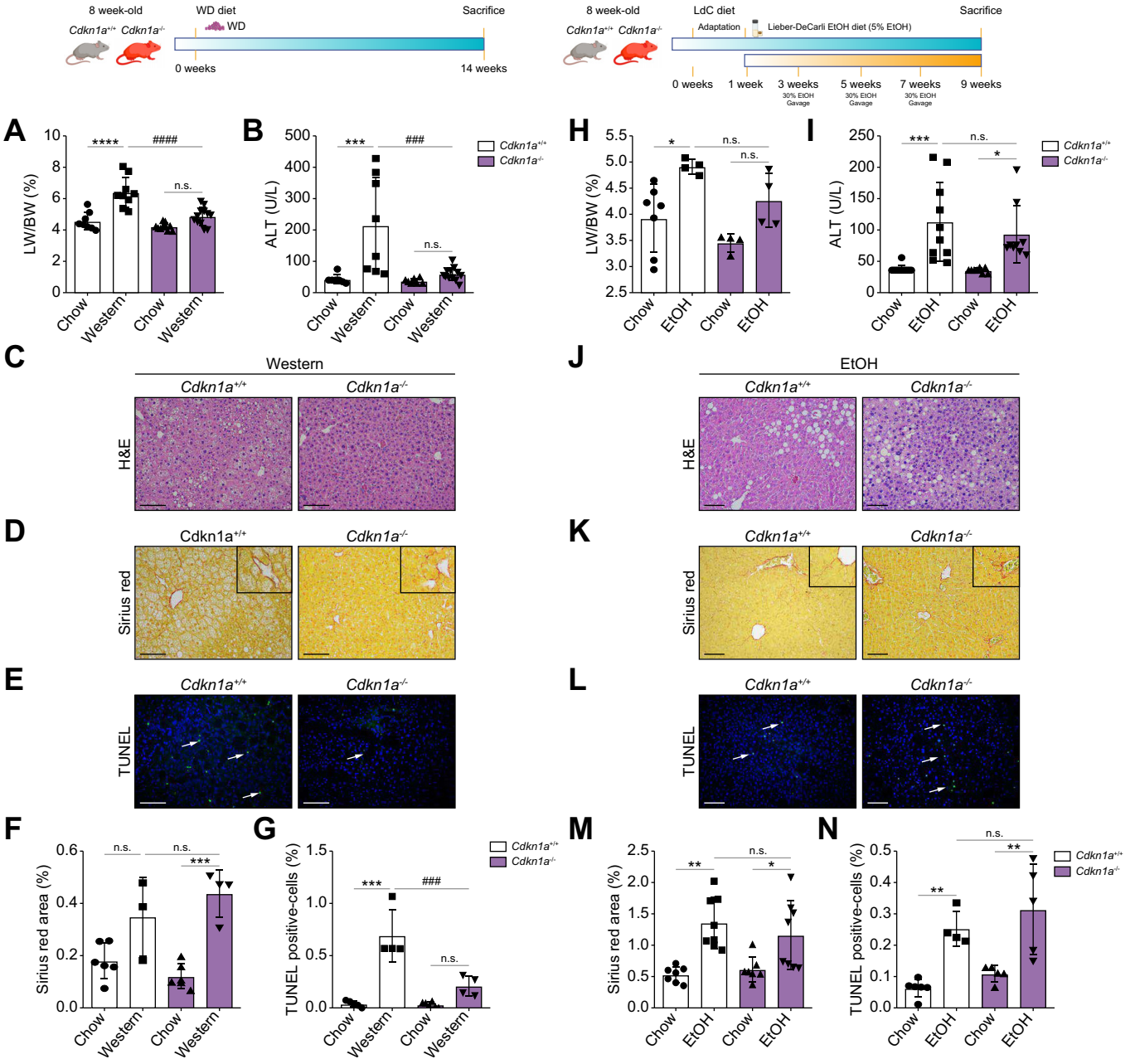

Fig. 3. Deletion of *Cdkn1a* in a preclinical model of SLD and in murine ALD. (Left panel) Schematic description of a WD model performed in of *Cdkn1a*$^{+/+}$ and *Cdkn1a*$^{-/-}$ mice. (A) LW/BW ratio (%). (B) ALT measurement in serum (n = 7–11). (C) H&E representative images in liver of *Cdkn1a*$^{+/+}$ and *Cdkn1a*$^{-/-}$ mice after WD. Scale bar = 100 μm. (D) Representative liver images stained with Sirius red (E) TUNEL staining was performed in liver cryosections of *Cdkn1a*$^{+/+}$ and *Cdkn1a*$^{-/-}$ mice after WD and (F,G) quantification of positive Sirius Red-stained area and TUNEL-positive cells. Scale bar = 100 μm. (n = 8–12); one-way ANOVA with *post hoc* Tukey test was used for the calculations (intragroup: ****p* <0.001, *****p* <0.0001; intergroup $^{\#\#\#}p$ <0.001, $^{\#\#\#\#}p$ <0.0001). (Right panel) Schematic description of an LdC model plus multiple binges performed in *Cdkn1a*$^{+/+}$ and *Cdkn1a*$^{-/-}$ mice. (H) LW/BW ratio (%). (I) ALT measurement in serum. (J) H&E staining in *Cdkn1a*$^{+/+}$ and *Cdkn1a*$^{-/-}$ mice after LdC EtOH diet. Scale bar = 100 μm. (I) Sirius Red staining performed in liver of *Cdkn1a*$^{+/+}$ and *Cdkn1a*$^{-/-}$ mice after LdC EtOH diet. Scale bar = 100 μm. (J) TUNEL staining was performed in liver cryosections of liver of *Cdkn1a*$^{+/+}$ and *Cdkn1a*$^{-/-}$ mice after LdC EtOH diet. Scale bar = 100 μm. (M,N) Quantification of Sirius Red-positive area and TUNEL-positive cells was done and graphed, respectively. n = 7–8; one-way ANOVA with *post hoc* Tukey test was used for the calculations (intragroup: **p* <0.05, *****p* <0.0001). ALD, alcohol-related liver disease; ALT, alanine aminotransferase; BW, body weight; *Cdkn1a*, cyclin-dependent kinase inhibitor 1A; EtOH, ethanol; LdC, Lieber-DeCarli; LW, liver weight; SLD, steatotic liver disease; WD, Western diet.

of this enzyme after LdC in both *Cdkn1a*$^{+/+}$ and *Cdkn1a*$^{-/-}$ mice (Fig. S7C). Liver histology analyses showed obvious macro and microsteatosis in the livers of all LdC-fed mice, often accompanied by the presence of inflammatory cells and necrosis (Fig. 3J, Fig. S7D).

Next, we measured deposition of extracellular matrix and liver fibrosis as a consequence of LdC feeding, using Sirius Red staining. Both *Cdkn1a*$^{+/+}$ and *Cdkn1a*$^{-/-}$ fed a LdC, displayed increased fibrogenesis, compared with control diet-fed mice (Fig. 3K,M, Fig. S7E,F), albeit no differences between both

strains were found. Concomitantly, we next evaluated cell death and compensatory proliferation in response to the increased inflammatory response. TUNEL- and Ki67-positive cells were increased in LdC-fed mice, compared with control diet-fed mice (Fig. 3L–N, Fig. S7G–I).

Altogether, these results evidenced that deletion of *Cdkn1a* did not protect against preclinical ALD.

Senescence is attenuated in *Cdkn1a*$^{-/-}$ animals fed a DuAL diet

Next, we investigated the induction of senescence associated to CDKN1A. Senescence-inducing signals activate transcriptional cascades which culminate in the activation of CDKN1A/p21-p53-p16 signaling resulting in irreversible cell cycle arrest.[23] Thus, we first analyzed mechanisms of cellular senescence in *Cdkn1a*$^{+/+}$ and *Cdkn1a*$^{-/-}$ mice, fed a DuAL diet. Interestingly, *Cdkn1a*$^{-/-}$ mice displayed a significant down-regulation in CDKN1A/p21 and p53 mRNA levels compared with *Cdkn1a*$^{+/+}$ mice (Fig. 4A,B). Although a tendency towards increased telomere shortening in *Cdkn1a*$^{+/+}$ fed a DuAL diet, no significant changes were observed between *Cdkn1a*$^{+/+}$ and *Cdkn1a*$^{-/-}$ mice (Fig. 4C).

Senescence can be also driven by other factors including DNA damage and reactive oxygen species (ROS). Both the phosphorylation of histone H2AX (γH2AX), a marker of DNA

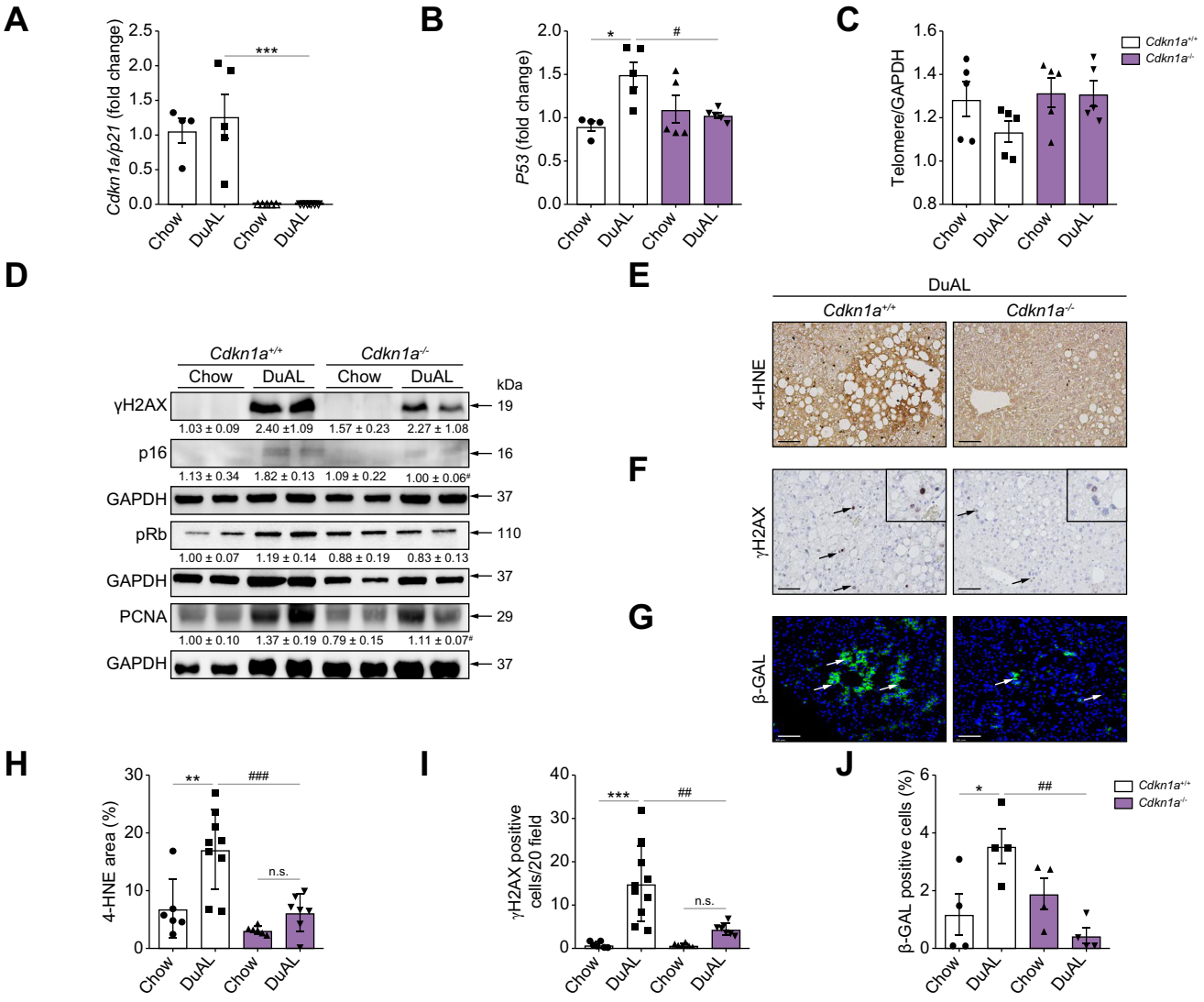

Fig. 4. Amelioration of liver senescence is characteristic of *Cdkn1a*$^{-/-}$ mice fed a DuAL diet. *Cdkn1a/p21* (A) and *P53* (B) mRNA relative liver expression to *Gapdh* was analyzed in *Cdkn1a*$^{+/+}$ and *Cdkn1a*$^{-/-}$ mice after DuAL diet. (C) Relative telomere length was calculated using PCR. (D) Total liver protein (two individuals' samples from each group are shown as representative of the group) were isolated from DuAL diet-fed *Cdkn1a*$^{+/+}$ and *Cdkn1a*$^{-/-}$ mice and analyzed for γH2AX, pRb, p16, and PCNA. Protein expression levels were normalized to the levels of total GAPDH and the ratio was calculated. (E–G) Representative liver sections of *Cdkn1a*$^{+/+}$ and *Cdkn1a*$^{-/-}$ mice stained with 4-HNE (E), γH2AX (F) and β-GAL (G). Scale bar = 100 μm. (H–J) Quantification of 4-HNE, γH2AX and β-GAL-positive cells per field. One-way ANOVA with *post hoc* Tukey test was used for the calculations. n = 6–10 (intragroup: ***p <0.001, ***p <0.001; intergroup: $^{\#}p$ <0.01, $^{\#\#\#}p$ <0.001). β-Gal, beta galactosidase; γH2AX, gamma H2A histone family member X; 4-HNE, 4-hydroxynonenal; *Cdkn1a*, cyclin-dependent kinase inhibitor 1A; DuAL, metabolic dysfunction-associated fatty liver disease and alcohol-related liver; *Gadph*, glyceraldehyde-3-phosphate dehydrogenase; pRb, phospho retinoblastoma tumor suppressor; PCNA, proliferating cell nuclear antigen.

damage and 4-hydroxynonenal (4-HNE) – a marker of lipid peroxidation – revealed less γH2AX and 4-HNE expression in *Cdkn1a*$^{-/-}$ compared with *Cdkn1a*$^{+/+}$ livers, after a DuAL diet (Fig. 4D–F,H,I, Fig. S8A,B). We further tested other markers of cellular senescence such as p16, which acts through the retinoblastoma (Rb) triggering cell cycle arrest and, therefore, decreased cell proliferation (Fig. 4D). P16, pRb, and PCNA were underexpressed in *Cdkn1a*$^{-/-}$ compared with *Cdkn1a*$^{+/+}$ animals (Fig. 4D). Moreover, immunofluorescence for the detection of β-galactosidase (β-GAL) activity, a widely used biomarker of cellular senescence, was significantly lower in *Cdkn1a*$^{-/-}$ compared with *Cdkn1a*$^{+/+}$ livers (Fig. 4G,J, Fig. S8C).

Inflammation is reduced in *Cdkn1a*$^{-/-}$ mice in experimental MetALD

Increased cellular senescence and the activation of the CDKN1A pathway act together to generate a proinflammatory environment, having a crucial role in propagating senescence and in the recruitment of immune cells to the senescent tissue.[24] In fact, *Cdkn1a* knockout animals showed a significant reduction in the accumulation of leukocytes (CD45^{+} cells) and infiltrated cells (CD11b^{+} cells), in contrast to *Cdkn1a*$^{+/+}$ mice, analyzed by immunofluorescence staining after a DuAL and a WD, but not after LdC diet (Fig. 5A–D, Fig. S8D–G). Furthermore, circulating F4/80^{hi}Ly6C^{hi} monocytes were significantly decreased in DuAL diet-fed *Cdkn1a*$^{-/-}$ compared with *Cdkn1a*$^{+/+}$ mice (Fig. 5E). Additionally, a clear trend towards decreased levels of mRNA transcripts for *Tnfα* and *Il6,* and significant downregulation in *Il1α* and *Il8* was found in *Cdkn1a*$^{-/-}$ mice, fed a DuAL diet (Fig. 5F–I).

We next measured typical markers of SASP such as insoluble factors (*Pge2*) and non-protein molecules (*Igfbp2*) which showed a significant reduction in *Cdkn1a*$^{-/-}$, compared with *Cdkn1a*$^{+/+}$ mice (Fig. 5J,K).

All these data indicated that *Cdkn1a*$^{-/-}$ mice displayed less inflammation and decreased proinflammatory secretome.

Examining the function of *Cdkn1a* in modulating lipid metabolism in experimental models of SLD

Senescence is linked to cell cycle arrest, oxidative stress, DNA damage and inflammation, and high expression of *Cdkn1a*, which triggers metabolic dysfunction. These alterations have been linked to promote the synthesis of genes involved in metabolism.[25]

Given the protection observed in steatosis, ballooning, lobular inflammation, fibrosis, and NAS in mice with

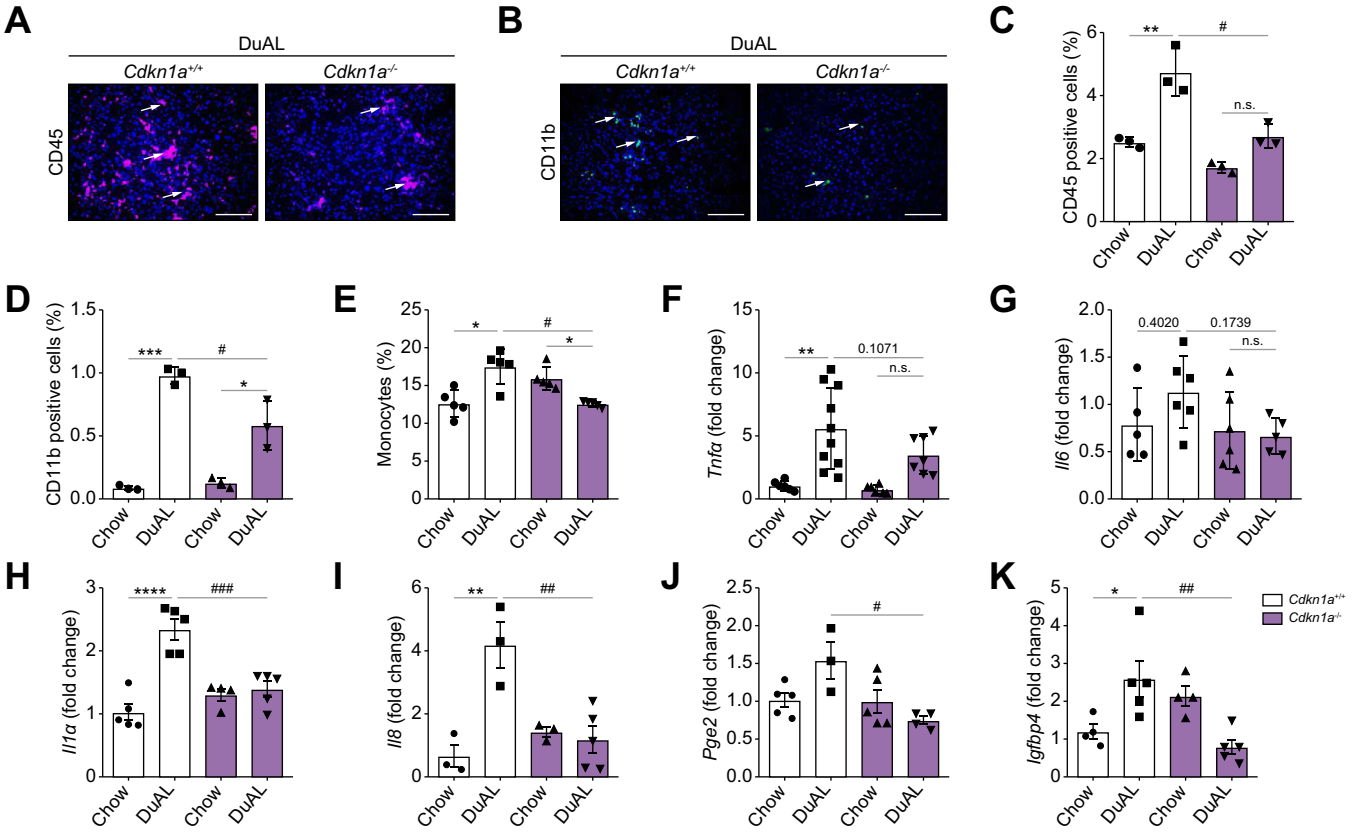

Fig. 5. Inflammation is significantly reduced in *Cdkn1a*$^{-/-}$ mice fed a DuAL diet. (A,B) Representative immunofluorescence staining for CD45 (A) and CD11b (B) in DuAL diet-fed *Cdkn1a*$^{+/+}$ and *Cdkn1a*$^{-/-}$ mice. Quantification of CD45- (C) and CD11b- (D) positive cells in the same samples. Arrows (→) indicate positive cells. (E) Circulating F4/80^{hi}Ly6C^{hi} cells in DuAL diet-fed *Cdkn1a*$^{+/+}$ and *Cdkn1a*$^{-/-}$ mice. *Tnfα* (F), *Il6* (G), *Il1α* (H), *Il8* (I), *Igfbp4* (J), and *Pge2* (K) mRNA expression determined by qPCR and normalized to the amount of *Gapdh* in the liver of DuAL-fed mice and controls. n = 4–10; one-way ANOVA with *post hoc* Tukey test was used for the calculations; intragroup: $^{**}p$ <0.01, $^{****}p$ <0.0001; intergroup: $^{\#}p$ <0.05, $^{\#\#\#}p$ <0.001. *Cdkn1a*, cyclin-dependent kinase inhibitor 1A; DuAL, metabolic dysfunction-associated fatty liver disease and alcohol-related liver; *Igfbp4*, Insulin like growth factor binding protein 4; *Gadph*, glyceraldehyde-3-phosphate dehydrogenase; *Pge2*, prostaglandin E2; qPCR, quantitative PCR; *Tnfα*, tumor necrosis factor alpha.

constitutive deletion of *Cdkn1a*, compared with *Cdkn1a*$^{+/+}$ animals, when fed a DuAL diet and a WD diet, but not a LdC diet (Fig. S9A–O), we next studied lipid accumulation measured by Oil Red O (ORO) staining and hepatic triglyceride (TG) content in the different preclinical models of SLD. Our results showed a significant increase in both, lipid accumulation measured by ORO and quantification, and hepatic TGs, in *Cdkn1a*$^{+/+}$ fed a DuAL or a WD diet (Fig. 6A–F, Fig. S10A,B); whilst *Cdkn1a*$^{-/-}$ mice exhibited a significant decrease in these parameters (Fig. 6A–F, Fig. S10A,B). No differences in ORO staining and liver TGs were observed between *Cdkn1a*$^{-/-}$ and *Cdkn1a*$^{+/+}$ fed an LdC diet (Figs. S10C–E). Therefore, we focused on the DuAL model to understand changes in metabolism regulated by *Cdkn1a*.

As lipid metabolism was affected by *Cdkn1a* deletion, we further explored genes and enzymes that play a pivotal role in that process. Although no differences were found in serum TGs between *Cdkn1a*$^{-/-}$ and *Cdkn1a*$^{+/+}$(Fig. 6G), the DuAL diet triggered significant increases in the number of transcripts of lipid and free fatty acid oxidation (FAO) genes including *Pparα* and *Fxr1* in *Cdkn1a*$^{-/-}$ compared with *Cdkn1a*$^{+/+}$ animals (Fig. 6H,I). Moreover, attenuation of *Pparγ, Cd36*, and *Fas*, genes related to FAO uptake, and *de novo* lipogenesis (DNL) was observed in *Cdkn1a*$^{-/-}$ compared with *Cdkn1a*$^{+/+}$ mice, fed a DuAL diet (Fig. 6J–L).

Moreover, glucose metabolism was unaltered because the mRNA transcripts of *Pepck* and *Pc* expression showed no differences between the experimental groups (Figs. S10F and G).

As AMPK plays a major role in the control of metabolism,[26] we subsequently analyzed the expression of pAMPK. Interestingly, AMPK activation in *Cdkn1a*$^{-/-}$ livers was significantly higher than in *Cdkn1a*$^{+/+}$ mice, fed a DuAL diet (Fig. 6N). Concomitantly, protein expression of AKT, which negatively regulates AMPK activation,[27] was significantly decreased in *Cdkn1a*$^{-/-}$ livers (Fig. 6N). Finally, SIRT3, a recently described key regulator in SLD whose deficiency aggravates this disease,[28] was significantly overexpressed in *Cdkn1a*$^{-/-}$ livers of mice fed a DuAL diet (Fig. 6N). The activation of AMPK – together with the phosphorylation/inhibition of acetyl-CoA carboxylase 2 – is believed to be the principal pathway regulating FAO.[29] Thus, we measured FAO (acid-soluble metabolites [ASM] + CO_2) which also indicated significantly higher concentration of FAO in liver tissue of *Cdkn1a*-deleted mice fed a DuAL diet (Fig. 6O, Fig. S10H,I). Altogether, our data showed that *Cdkn1a* deletion improved preclinical SLD by increasing FAO and decreasing free fatty acid (FFA) uptake and DNL. Mechanistically, activation of AMPK and SIRT3, in the absence of AKT phosphorylation, was associated with improved lipid homeostasis in *Cdkn1a*-deficient animals.

Lipid balance is dysregulated in *Cdkn1a*-deficient hepatocytes

Because metabolic dysfunction was characteristic of MASLD preclinical models, we further investigated the specific cell type involved in the process. For this purpose, we first isolated primary hepatocytes from C57BL6/J mice and silenced *Cdkn1a* expression by siRNA. Lack of *Cdkn1a* mRNA transcripts and protein expression was confirmed in silenced *Cdkn1a* (*siCdkn1a*) compared with control (*siLuc*) hepatocytes, by quantitative real-time PCR and Western blot, respectively (Fig. 7A,B). To initially assess glucose modulation of DNL modulated by *Cdkn1a*, we quantified the incorporation of glucose carbons into lipid fractions of *siLuc* and *siCdkn1a* hepatocytes, in the presence or absence of insulin. Compared with *siLuc* hepatocytes, the contribution of glucose to DNL was significantly decreased in *siCdkn1a* hepatocytes, especially after insulin stimulation (Fig. 7C).

Hepatic lipogenesis is largely regulated at the transcriptional level by two transcription factors: the sterol regulatory element-binding protein-1c (SREBP1c) and the carbohydrate response element binding protein (ChREBP), which have overlapping target genes and mediate the input from insulin and glucose, respectively.[30] Thus, we performed measurements in hepatocytes in response to glucose without insulin stimulation. As expected, a substantial decrease in the mRNA abundance of the lipogenic genes, *Srebp1c* and *Chrebp1*, was observed in *siCdkn1a*-knockdown hepatocytes (Fig. 7D,E). To corroborate our findings obtained with siRNA, we next isolated primary hepatocytes from *Cdkn1a*$^{+/+}$ and *Cdkn1a*$^{-/-}$ animals and performed ORO staining pictures, which showed a reduction in the accumulation of lipid droplets in *Cdkn1a*$^{-/-}$ mice compared with wild type *Cdkn1a*$^{+/+}$ (Fig. 7F,G).

To further understand if activation of AMPK and SIRT3, in the absence of AKT phosphorylation, was associated with improved lipid homeostasis, we evaluated its expression in primary hepatocytes isolated from *Cdkn1a*$^{+/+}$ and *Cdkn1a*$^{-/-}$ animals (Fig. 7H). Interestingly, we observed increased significant SIRT1 overexpression in hepatocytes isolated from *Cdkn1a*$^{-/-}$ compared with *Cdkn1a*$^{+/+}$ animals. No differences were observed in AMPK expression, but a clear trend towards decreased AKT phosphorylation in *Cdkn1a* KO primary hepatocytes. Altogether, these data further supported our *in vivo* findings, indicating reduced lipogenesis in *Cdkn1a*-deleted primary hepatocytes *in vitro.*

CDKN1A inhibition using palbociclib ameliorated liver injury and restored hepatic metabolism in advanced SLD

Based on the possible role of CDKN1A in preclinical MASLD, we subsequently explored the therapeutic value of CDKN1A inhibition. Therefore, a DuAL diet for 10 weeks was fed in presence of palbociclib (100 mg/kg), a well-known cyclin-dependent kinase 4/6 (CDK4/6) inhibitor.[31,32] As expected, palbociclib significantly downregulated the mRNA levels of *Cdkn1a*, *p53*, *Cyclin A2*, and *B1* (Fig. 8A–D). Interestingly, palbociclib-treated animals displayed a reduction in steatosis, ballooning, and inflammation accompanied by a significant decrease in LW/BW ratio and significantly enhanced serum markers of liver injury (e.g. AST), compared with DuAL-fed animals (Fig. 8E–G).

As the DuAL diet triggers fiber deposition after 10 weeks of feeding,[21] we next evaluated liver fibrosis using Sirius Red staining. Concomitantly, a significant reduction in percentage of Sirius Red positive area was found in palbociclib-treated mice compared with DuAL-fed mice (Fig. 8H–J). Given the accumulating evidence of our preclinical data indicating that lipid accumulation was impaired as a result of *Cdkn1a* function, ORO staining was performed. Although ORO was more

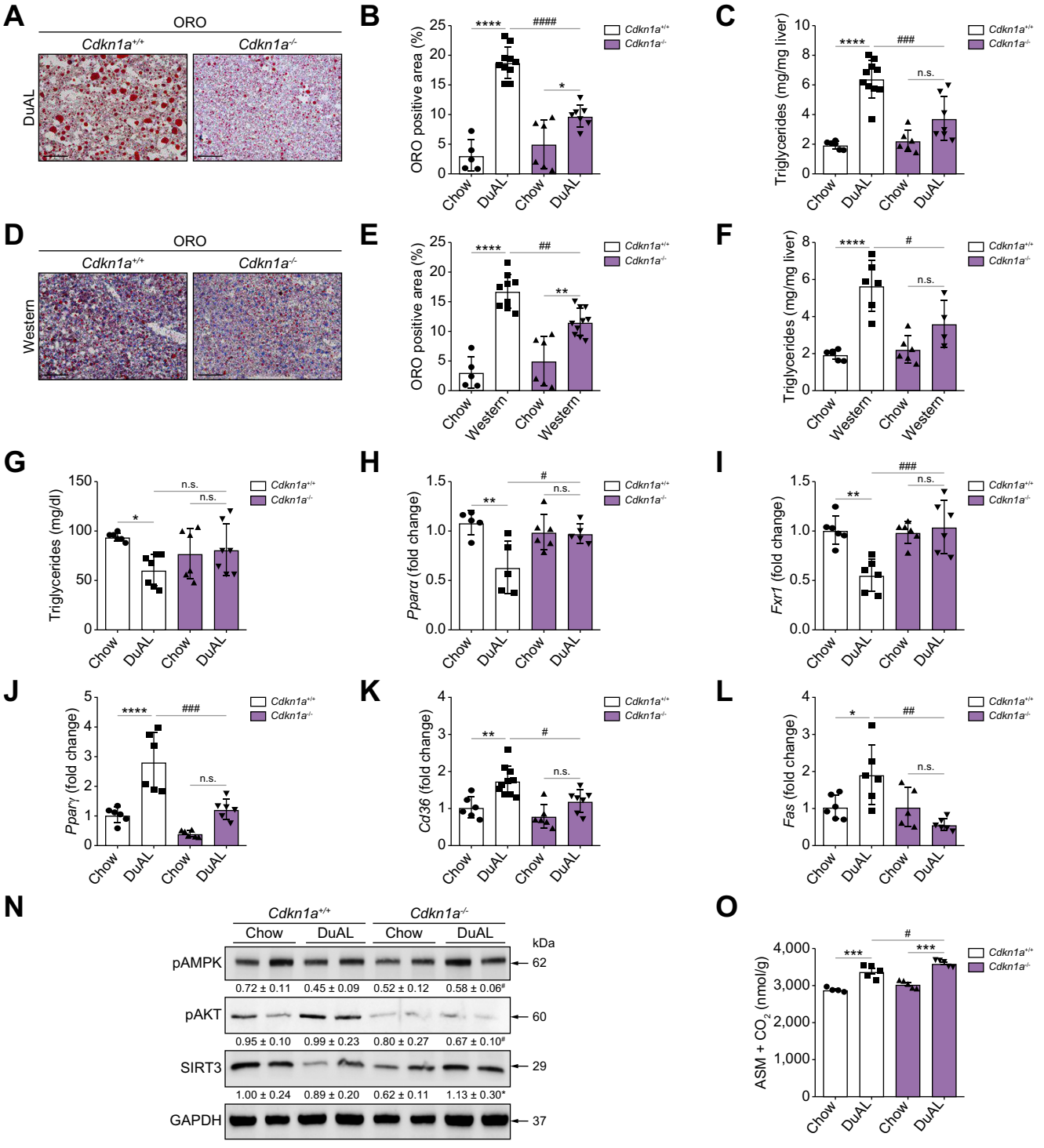

Fig. 6. Lipid metabolism in experimental models of SLD and MetALD. (A) ORO staining performed in liver cryosection of DuAL-fed mice and (B) each quantification. Scale bar = 100 μm. (C) Quantification of hepatic triglycerides after DuAL diet (mg/mg liver). (D) Illustrative ORO-stained liver sections from each group of mice after WD. Scale bar = 100 μm. (E) Quantification of ORO-stained area (n = 5–10) (F) Quantification of hepatic triglycerides after a WD in *Cdkn1a*$^{+/+}$ and *Cdkn1a*$^{-/-}$ after WD and controls was done and graphed. (G) Serum triglycerides levels after a DuAL diet and controls (mg/dl). (H) *Pparα*, (I) *Fxr1*, (J) *Pparγ*, (K) *Cd36*, and (L) *Fas* mRNA expression determined by qPCR and normalized to the amount of *Gapdh* in liver of DuAL-fed mice and controls. (N) Total liver protein (two individuals' samples from each group are shown as a representative of the group) were isolated from DuAL diet-fed *Cdkn1a*$^{+/+}$ and *Cdkn1a*$^{-/-}$ mice and analyzed for pAMPK, pAKT, and SIRT3. GAPDH was used as a loading control. (O) FAO was measured in liver tissue of DuAL diet-fed *Cdkn1a*$^{+/+}$ and *Cdkn1a*$^{-/-}$ mice and the concentration of ASM + CO_2 (mmol/g) was quantified and graphed. n = 6–10, one-way ANOVA with *post hoc* Tukey test was used for the calculations; intragroup: $^{*}p$ <0.05, $^{****}p$ <0.0001; intergroup: $^{\#}p$ <0.05, $^{\#\#\#\#}p$ <0.0001. ASM, acid-soluble metabolites; CO_2, carbon dioxide; *Cdkn1a*, cyclin-dependent kinase inhibitor 1A; DuAL, metabolic dysfunction-associated fatty liver disease and alcohol-related liver; FAO, fatty acid oxidation; *Fxfr1*, fragile X-related protein 1; *Gadph*, glyceraldehyde-3-phosphate dehydrogenase; MetALD, metabolic-associated alcoholic liver disease; ORO, Oil Red O; qPCR, quantitative PCR; *Pprα*, peroxisome proliferation-activated receptor alpha; *Pparγ*, peroxisome proliferation-activated receptor gamma; SLD, steatotic liver disease; WD, Western diet.

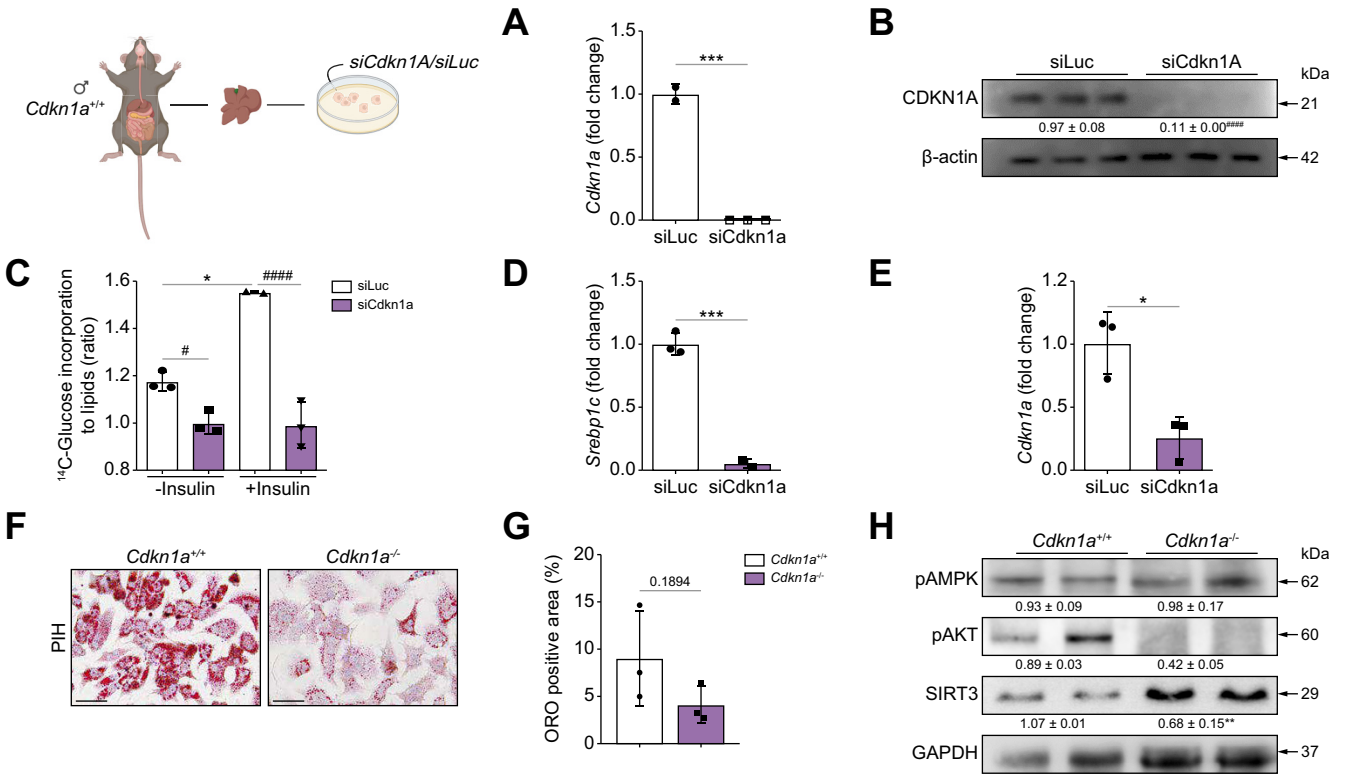

Fig. 7. Lipid balance is dysregulated in *Cdkn1a*-deficient hepatocytes. A schematic description of *siRNA* transfection is shown. (A) *Cdkn1a* mRNA relative expression to *Gapdh* in *siLuc* and *siCdkn1a* hepatocytes. (B) Comparative protein expression of CDKN1A in *siLuc* and *siCdkn1a* hepatocytes by immunoblotting analysis. β-ACTIN was used as a loading control. Ratio between CDKN1A and β-ACTIN was calculated. (C) Incorporation of glucose into lipid fractions of *siLuc* and *siCdkn1a* hepatocytes treated with 0.25 uCi of D-[^{14}C(U)] glucose overnight. Data are presented as ratio of labeled glucose incorporation to lipids. (D) *Srebp1c* and (E) *Chrebp1* mRNA relative expression to *Gapdh* in *siLuc* and *siCdkn1a* hepatocytes. Statistical significance between *siCtrl* and *siCdkn1a* primary hepatocytes in qPCR assays was determined by Student *t* test (*p <0.05). (F) ORO staining performed in primary hepatocytes isolated from *Cdkn1a*$^{+/+}$ and *Cdkn1a*$^{-/-}$. (G) quantified in a graph and (H) protein expression for pAMPK, pAKT, and SIRT3 was studied in primary hepatocytes isolated from *Cdkn1a*$^{+/+}$ and *Cdkn1a*$^{-/-}$ mice (two individuals' samples from each group are shown as a representative of the group). GAPDH was used as a loading control. Scale bar = 50 μm. n = 3, one-way ANOVA with *post hoc* Tukey test was used for the calculations, intragroup: *p <0.05; ***p <0.001; intergroup: #p <0.05, ####p <0.0001). AMPK, AMP-activated protein kinase; AKT, serin/theonine kinase 1; *Cdkn1a*, cyclin-dependent kinase inhibitor 1A; *Gadph*, glyceraldehyde-3-phosphate dehydrogenase; Luc, luciferase; ORO, Oil red O; PIH, Primary hepatocytes isolated; qPCR, quantitative PCR; SIRT3, sirtuin 3.

pronounced in DuAL-fed animals, no differences with palbociclib-treated mice were observed (Fig. 8J,K).

Collectively these data suggested that CDKN1A pharmacological inhibition protected against preclinical SLD with metabolic dysfunction alone or combined with harmful alcohol consumption.

Discussion

The prevalence of MASLD is rapidly increasing (exceeding 80% in morbidly obese individuals).[33] MASLD ranges from non-alcoholic fatty liver (NAFL) in the case of isolated steatosis to MASH, fibrosis, cirrhosis, and end-stage HCC. There is a lack of effective treatment options to tackle this disease, which is already posing a global threat on public health and economy. However, to achieve progress, the complex pathophysiology of MASLD needs to be investigated in depth.

In the past decade, the role of cellular senescence in the development of MASLD and its progression towards MASH has garnered considerable interest. Cellular senescence refers to the arrest of the cell cycle associated to specific phenotypic changes, including the release of SASP.[23] Hepatocyte senescence is a central pathomechanism as it may foster intracellular fat accumulation, fibrosis, and inflammation. In fact, during metabolic dysfunction, cellular senescence is favored further perpetuating metabolic dysregulation.

Increased expression of cell cycle inhibitors including *Cdkn1a* is characteristic of hepatocyte senescence.[34] Importantly, *CDKN1A/P21* expression was shown to increase in the livers of individuals with MASLD and increases with disease progression.[15] Moreover, *CDKN1A* is upregulated during inflammation and fibrosis in CLD, including in end-stage HCC.[35–37] Concomitantly, we did not only observe increased expression of *CDKN1A* for patients with high NAS and fibrosis scores, but also identified increased gene counts for *CDKN1A* in patients with early and intermediate stages of liver disease, and in patients with advanced CLD, including cirrhosis. Importantly, we found a correlation between *CDKN1A* expression and more advanced stages (or higher counts on steatohepatitis and fibrosis) in patients with SLD and proved its performance as a biomarker, thus underscoring the potential of CDKN1A (or its protein P21) as a prognostic marker for SLD in liver tissue. In our study, we performed CDKN1A/p21 IHC in patients with MASH and observed that CDKN1A expression was restricted to hepatocyte nuclei and not found in any other

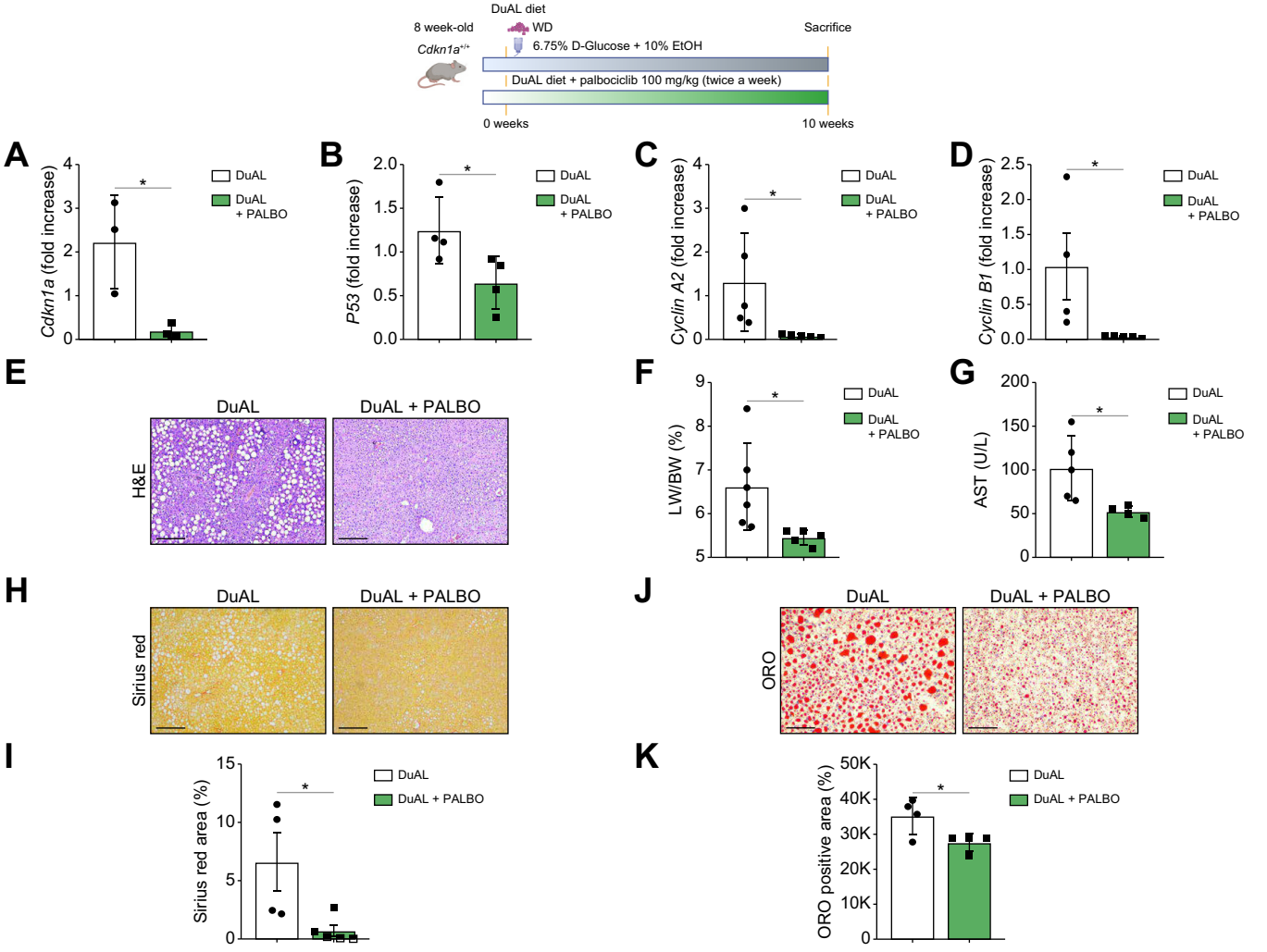

Fig. 8. The inhibition of CDK4/6 protects mice from liver injury in advanced SLD. Schematic description of a DuAL model plus oral palbociclib administration performed in wild type BL/6 mice. (A) *Cdkn1a*, (B) *p53*, (C) *Cyclin A2*, and (D) *Cyclin B1* mRNA expression determined by qPCR and normalized to the amount of *Gapdh* in liver of DuAL-fed mice and controls. (E) H&E staining in liver of DuAL-fed mice and controls was performed. Scale bar = 100 μm. (F) LW/BW ratio (%). (G) AST measurement in serum. (H) Sirius red staining was performed in livers of DuAL-fed mice and controls, and quantification was represented (I). Scale bar = 100 μm. (J) ORO staining was performed in liver cryosections of DuAL-fed mice and controls, and quantification was graphed (K). n = 5–6, Student *t* test was used for the calculations, **p* <0.05. AST, aspartate amino transferase; CDK4/6, cyclin-dependent kinase 4/6; *Cdkn1a*, cyclin-dependent kinase inhibitor 1A; DuAL, metabolic dysfunction-associated fatty liver disease and alcohol-related liver; *Gadph*, glyceraldehyde-3-phosphate dehydrogenase; LW/BW, liver weight/body weight; ORO, Oil Red O; qPCR, quantitative PCR; SLD, steatotic liver disease.

liver cell types, as previously reported.[15,38] However, as observed in liver mouse isolated cells, the expression and role of CDKN1A in NPCs (e.g. HSCs, KCs) need to be further investigated.

Another clear association between senescence and MASLD comes from the use of animal models. As many patients with SLD exhibit an alcohol drinking pattern, we chose to use this recently novel preclinical model developed in our laboratory.[21] The DuAL model triggers stress factors including liver injury, oxidative stress, and lipid and DNA damage, that lead to premature senescence induced DNA damage as observed by the phosphorylation of γH2AX and subsequently contributing to cell cycle arrest by stimulating the expression of *Cdkn1a* and the activation of P16. P16-mediated senescence acts through the Rb pathway inhibiting the action of the CDKs leading to G1 cell cycle arrest and proliferation. Specifically, *Cdkn1a* binds to *CcnA/Cdk2* and *CcnE/Cdk2* and complexes among others, thereby preventing progression from G_1-to S-phase. Interestingly DuAL-fed *Cdkn1a* knockout animals displayed a significant downregulation of *CcnA2* and *D1* but not of *E1*, the latter most likely because of increased activity of other cell cycle inhibitors such as pP27 and P18, as reported earlier.[39] Interestingly, *Cdkn1a*$^{-/-}$ mice were protected against DuAL-derived cellular senescence.

Senescent cells release the SASP, a proinflammatory secretome that contributes to tissue dysfunction in both an autocrine and paracrine fashion.[23] A more proinflammatory SASP was detected in DuAL-fed animals via the significant upregulation of membrane-bound IL1α which acts in an autocrine fashion triggering the production of *Il6* and *Il8*. Interestingly, we observed a positive correlation for *IL6ST* and *IL8* in the MASLD cohort. Moreover, the SASP stimulates the immune

system to clear senescent cells triggering cell death, but can also reinforce or even maintain the senescent cell state, thereby contributing to persistent chronic inflammation.[23] Of note, loss of *Cdkn1a* ameliorated cell death – both necrotic and apoptotic. It is well-known that *Cdkn1a* can protect cells against apoptosis, given its transcriptional regulation through protein–protein interaction or DNA repair activity.[40]

DuAL mice elicited increased presence of circulating monocytes and hepatic lymphoid and myeloid cells. Overall, loss of *Cdkn1a* ameliorated the senescence-associated proinflammatory state of DuAL-fed mice and prevented fibrosis.

Other experimental models were used to further understand the etiopathogenic factors contributing to the role of CDKN1A in MASLD. Therefore, we subsequently applied a model of WD alone. Again, *Cdkn1a* knockout mice displayed protection against SLD in terms of markers of liver damage (ALT and AST), LW/BW ratio and lipid accumulation (ORO staining and hepatic TGs), and cell death (TUNEL staining). Although no differences were observed in liver fibrosis between $Cdkn1a^{+/+}$ and $Cdkn1a^{-/-}$ livers, it is tempting to speculate that a longer feeding period is needed to trigger HSC activation and extracellular matrix deposition in this model. Finally, we used the LdC model to understand the effects of ALD mediated by CDKN1A. However, loss of *Cdkn1a* did not exert a protective effect against ALD. These results indicated that metabolic alterations presented in DuAL mice and characteristic of SLD patients with harmful alcohol intake might be needed.

Therefore, next we studied metabolic dysfunction, strongly associated with cellular senescence. In fact, hepatocytic senescence was shown to impair hepatic mitochondrial β-oxidation, thereby hindering FFAs elimination and promoting TG accumulation, and hepatic steatosis.[38,41] Importantly, both DuAL and WD-fed $Cdkn1a^{-/-}$ mice showed a dramatic reduction in lipid accumulation and hepatic TG content. Moreover, β-oxidation in DuAL-fed *Cdkn1a* knockout mice was demonstrated by increased expression of *Pparα* and *Fxr1*. These results were linked with reduced expression of genes associated with FFA uptake such as *Pparγ*, *Cd36*, and *Fas* in DuAL-fed $Cdkn1a^{-/-}$ animals. As earlier studies in L02 cells revealed that *CDKN1A* might play a role in lipid metabolism in human hepatocytes,[42] we next isolated primary hepatocytes and performed functional assays using *siCdkn1a*. Our data showed that *Srebp1c and Chrebp* mRNA expression in *siCdkn1a*-treated murine primary hepatocytes indicated decreased lipogenesis, further supported by decreased lipid deposition in $Cdkn1a^{-/-}$ primary hepatocytes. Hence, for the first time our findings provide a link between CDKN1A and lipid accumulation in hepatocytes. Moreover, systemic clearance of P16-expressing cells or administration of a senolytic drug cocktail were reported to decrease hepatocytic senescence and ameliorated hepatic steatosis.[38,41]

AMPK and AKT are two primary effectors in response to metabolic stress. Whilst AMPK acts as an energy-sensing factor which rewires metabolism, AKT displays an antagonistic role.[43] Interestingly, we found that whereas AMPK activation was significantly higher in DuAL-fed *Cdkn1a*-deleted mice, AKT was abrogated in the absence of CDKN1A. Moreover, since SIRT3 is a down-stream protein of AMPK, we also studied its expression pattern. Interestingly, we found that AMPK-SIRT3 activation in *Cdkn1a*-deficient animals protected against metabolic stress. Because AMPK controls DNL that generates malonyl-CoA, which, in turn, regulates FAO,[44] we next confirmed that the concentration of FAO (ASM + CO_2) in *Cdkn1a*-deleted liver tissue was associated with increased FAO in these animals.

Considering these data, how can CDKN1A regulate lipid metabolism? The answer might imply the link between cellular senescence and mitochondria. In patients with MASLD, metabolic dysregulation as a consequence of senescence occurs in the liver, but its consequences expand to the adipose tissue and the pancreas, leading to insulin resistance and inflammation. Mechanistically, stress factors such as ROS (or the formation of advanced glycation end-products) trigger hepatocyte senescence by one or several of the following mechanisms: (i) increasing the expression of CDKN1A;[45] (ii) lipids (ceramide or sphingosine) specifically upregulate *p21* expression;[46] (iii) impairing mitochondrial β-oxidation causing further production of ROS, DNA damage, and changes in mitochondrial function, dynamics, and morphology, and/or (iv) modulating AMPK activation via mitochondrial metabolites (NAD^+/NADH ratio) and consequently stabilizing CDKN1A or causing the phosphorylation of P53, decreased p38MAPK and NF-kB activity and the secretion of proinflammatory SASP factors, as previously suggested.[47]

Finally, we evaluated therapeutic avenues by exploring the use of CDKN1A inhibitors in DuAL-fed mice. For this purpose, we used palbociclib, an inhibitor of CDK4/6, and a specifically regulator of cellular transition from the G1 phase of the cell cycle to the S-phase.[48] Administration of palbociclib in DuAL-fed animals successfully decreased serum markers of liver damage, liver fibrosis, and lipid accumulation, conferring protection against preclinical MetALD. These results are consistent with the beneficial role of palbociclib in end-stage models of liver disease.[32]

However, the feasibility of translating these preclinical results to clinical practice are unknown. Although the use of palbociclib in combination with aromatase inhibitors in the therapy of postmenopausal women with metastatic breast cancer (ER^+, $HER2^-$) prolongs disease-free survival, the use of palbociclib in patients with CLD is supported in preclinical models as a single agent or in combination with other drugs, especially in end-stage liver disease.[32] Therefore, the identification of synergistic partners for palbociclib in CLD will allow stronger effects in the modulation of cellular senescence and apoptosis. Of note, in large clinical trials,[49,50] palbociclib has showed to be well tolerated and rarely mentioned serum ALT elevations or hepatotoxicity that improved on discontinuation and recurred rapidly when restarted.

In summary, in the present study we showed that the senescence marker CDKN1A might have a prognostic value in liver tissue of patients with metabolically induced SLD and fibrosis, with or without alcohol consumption. Moreover, we unveiled that *Cdkn1a* plays a pivotal role in cellular senescence that lead to inflammation and fibrosis by regulating lipid metabolism via β-oxidation and preventing FFA uptake. Mechanistically, activation of AMPK and SIRT3 and abrogation of AKT expression were linked to this effect. Finally, we showed that *Cdkn1a* inhibition might be a novel therapeutic avenue for patients with SLD, advocating for the potential of senotherapeutic drugs targeting cellular senescence as viable therapeutic options for treating SLD and MetALD.

Affiliations

[1]*Department of Immunology, Ophthalmology and ENT, Complutense University School of Medicine, Madrid, Spain;* [2]*12 de Octubre Health Research Institute (imas12), Madrid, Spain;* [3]*Department of Obstetrics and Gynaecology, The Affiliated Drum Tower Hospital of Nanjing University Medical School, Nanjing, China;* [4]*Institute of Nutrition and Food Technology (INTA), Universidad de Chile, Santiago, Chile;* [5]*Physiology Institute, Science Faculty, Universidad de Valparaíso, Valparaíso, Chile;* [6]*State University of Campinas, Campinas, Sao Paulo, Brazil;* [7]*Department of Anesthesiology, Nanjing Pukou District Hospital of Chinese Medicine Central Laboratory Affiliated to Nanjing University of Chinese Medicine, Nanjing, China;* [8]*Servicio de Aparato Digestivo, Hospital General Universitario Gregorio Marañón, Madrid, Spain;* [9]*Health Research Institute Gregorio Marañón (IiSGM), Madrid, Spain;* [10]*Centre for Biomedical Research, Network on Liver and Digestive Diseases (CIBEREHD), Madrid, Spain;* [11]*Department of Cancer Biology, Dana-Farber Cancer Institute, Boston, MA, USA;* [12]*Department of Cell Biology, Harvard Medical School, Boston, MA, USA;* [13]*Department of Physiology, Basque Country University (UPV/EHU) School of Medicine and Nursing, Bilbao, Spain;* [14]*Biobizkaia Health Institute, Barakaldo, Spain;* [15]*Servicio de Anatomía Patológica Hospital General Universitario Gregorio Marañón Madrid, Spain;* [16]*Liver Disease Laboratory, Center for Cooperative Research in Biosciences (CIC bioGUNE), Basque Research and Technology Alliance (BRTA), Derio, Bizkaia, Spain;* [17]*Department of Internal Medicine III, University Hospital, RWTH Aachen, Aachen, Germany;* [18]*Department of Biochemistry and Molecular Biology, Faculty of Pharmacy, Complutense University, Madrid, Spain;* [19]*San Carlos Health Research Institute (IdISSC), Madrid, Spain;* [20]*Instituto de Biomedicina de Sevilla, IBiS/Hospital Universitario Virgen del Rocío/CSIC/Universidad de Sevilla, Sevilla, Spain;* [21]*Liver Vascular Biology, IDIBAPS Biomedical Research Institute, Barcelona, Spain;* [22]*Department of Visceral Surgery and Medicine, Inselspital, Bern University Hospital, University of Bern, Bern, Switzerland;* [23]*Laboratorio de Plasticidad de Células Hepáticas y Reparación de Tejidos, Institut d'Investigacions Biomèdiques August Pi i Sunyer (IDIBAPS), Barcelona, Spain;* [24]*Liver Unit, Hospital Clinic, Barcelona, Spain;* [25]*Endocrinology Department, Vall d'Hebron University Hospital, Vall d'Hebron Institute for Research (VHIR), Barcelona, Spain;* [26]*Centre for Biomedical Research, Network on Diabetes and Associated Metabolic Disorders (CIBERDEM), Madrid, Spain;* [27]*Liver Unit, Vall d'Hebron University Hospital, Vall d'Hebron Institute for Research (VHIR), Barcelona, Spain;* [28]*Puerta de Hierro University Hospital, Instituto de Investigación Sanitaria Puerta de Hierro, Majadahonda, Madrid, Spain;* [29]*Hepatology Laboratory, Solid Tumors Program, CIMA, University of Navarra, Pamplona, Spain;* [30]*IdiSNA, Navarra Institute for Health Research, Pamplona, Spain;* [31]*Department of General and Digestive System Surgery, Virgen de la Arrixaca University Hospital, Murcia, Spain;* [32]*Experimental Pathology Service, Biomedical Research Institute of Murcia (IMIB), Murcia, Spain;* [33]*Laboratorio de Obesidad y Metabolismo, Instituto de Investigación Biomédica de Murcia (IMIB-Arrixaca), Murcia, Spain*

Abbreviations

4-HNE, 4-hydroxynonenal; ACLD, advanced chronic liver disease; ALD, alcohol-related liver disease; ALT, alanine aminotransferase; ASM, acid-soluble metabolites; AST, aspartate aminotransferase; AUROC, area under the receiver operating characteristic curve; BW, body weight; CC, compensated cirrhosis; CC3, cleaved-caspase-3; CC8, cleaved-caspase-8; CDK4/6, cyclin-dependent kinase 4/6; CDK, cyclin-dependent kinase; CDKN1A, cyclin-dependent kinase inhibitor 1A; CDKN, cyclin-dependent kinases inhibitors; ChREBP, carbohydrate response element binding protein; CLD, chronic liver disease; DC, decompensated cirrhosis; DNL, *de novo* lipogenesis; DuAL, metabolic dysfunction-associated fatty liver disease and alcohol-related liver; EtOH, ethanol; FFA, free fatty acid; FAO, fatty acid oxidation; GADPH, glyceraldehyde-3-phosphate dehydrogenase; GTT, glucose tolerance test; HCC, hepatocellular carcinoma; HSCs, hepatic stellate cells; IHC, immunohistochemistry; KCs, Kupffer cells; LdC, Lieber-DeCarli; LW, liver weight; MASH, metabolic-associated steatohepatitis; MASLD, metabolic dysfunction-associated steatotic liver disease; MetALD, metabolic-associated alcoholic liver disease; NAFL, non-alcoholic fatty liver; NAS, NAFLD Activity Score; NPC, non-parenchymal cells; ORO, Oil Red O; PCNA, proliferating cell nuclear antigen; qPCR, quantitative PCR; Rb, retinoblastoma; ROS, reactive oxygen species; SASP, senescence-associated secretory phenotype; SLD, steatotic liver disease; SR, Sirius Red; SREBP1c, sterol regulatory element-binding protein-1c; TGs, triglycerides; TUNEL, terminal deoxynucleotidyl transferase-mediated deoxyuridine triphosphate nick-end labeling; WD, Western diet.

Financial support

This work was supported by the MICIU/AEI/10.13039/501100011033 PID2020-113299RA-I00, PID2020-11782RB-I00, PID2020-117941RB-I00, PID2021-124425OB-I00, PID2023-150260OB-I00, and PID2023-151347OB-I00, all of which were co-financed with Fondos FEDER, UE, Basque Government, Department of Education (IT1476-2), the Institute of Health Carlos III (ISCIII) (awards numbers PI20/00505 and PI23/00171), EXOHEP2-CM (S2022/BMD-7409), HORIZON-HLTH-2022-STAYHLTH-02 under agreement No 101095679 and the Dynamic Resilience Program - Wellcome Leap. CSG is an Atracción de Talento (CAM) 2019 2019-T1/BMD-13313. The research group belongs to the validated Research Groups Ref. 970935 'Liver Pathophysiology', 920631 'Lymphocyte immunobiology', 920361 'Inmunogenética e inmunología de las mucosas' and IBL-6 (imas12-associated). ALP and AH are recipients of a UCM Real Colegio Complutense (RCC) Harvard - Santander scholarships CT17/17 and CT15/23, respectively. BRM is supported by the 'Miguel Servet Type I' program (CP19/00098, funded by the Institute of Health Carlos III, Spain; co-funded by the 'Fondo Europeo de Desarrollo Regional').

Conflicts of interest

The authors declare no conflicts of interest that pertain to this work.

Please refer to the accompanying ICMJE disclosure forms for further details.

Authors' contributions

Carried out the experimental and drafted the manuscript: AL-P, AH-G, FG. Performed experiments and helped with the animals' maintenance: GJ, LM-B, RB-U, MMes, OE-V, KZ, MMaz. Helped with primary isolated hepatocytes experiments: EV-O, EB-L, IA, BM. Contributed to the intellectual work and provided experimental techniques: BG-S, MA, TCD, MLM-C, MRM, ST, PI, PA. Provided pivotal intellectual input: JV, RB, EM-N, CS-G, MA-A. Performed all the histopathological analysis: MIP, CMM-C. Provided patients' cohorts: RG-D, DM-M, JA, MR-G, AM-A, DS-R, AF-I, JG-S, MC, IG, PG, AC, JR-E, JM-P, MD-F, BR-M. Supervised, analyzed the experiments, drafted and wrote the manuscript and provided the funding: PP, YAN, FJC.

Data availability statement

The experimental data sets generated and/or analyzed during the current study are available from the corresponding author upon reasonable request.

Supplementary data

Supplementary data to this article can be found online at https://doi.org/10.1016/j.jhepr.2024.101230.

References

Author names in bold designate shared co-first authorship

[1] Kreis NN, Louwen F, Yuan J, et al. The multifaceted p21 (Cip1/Waf1/CDKN1A) in cell differentiation, migration and cancer therapy. Cancers (Basel) 2019;11:1220.

[2] Sherr CJ, Roberts JM. CDK inhibitors: positive and negative regulators of G1-phase progression. Genes Dev 1999;13:1501–1512.

[3] Waga S, Hannon GJ, Beach D, et al. The p21 inhibitor of cyclin-dependent kinases controls DNA replication by interaction with PCNA. Nature 1994;369:574–578.

[4] Engeland K. Cell cycle arrest through indirect transcriptional repression by p53: I have a DREAM. Cell Death Differ 2018;25:114–132.

[5] d'Adda di Fagagna F. Living on a break: cellular senescence as a DNA-damage response. Nat Rev Cancer 2008;8:512–522.

[6] Engelmann C, Tacke F. The potential role of cellular senescence in non-alcoholic fatty liver disease. Int J Mol Sci 2022;23:652.

[7] Papatheodoridi AM, Chrysavgis L, Koutsilieris M, et al. The role of senescence in the development of nonalcoholic fatty liver disease and progression to nonalcoholic steatohepatitis. Hepatology 2020;71:363–374.

[8] Asrani SK, Devarbhavi H, Eaton J, et al. Burden of liver diseases in the world. J Hepatol 2019;70:151–171.

[9] Paik JM, Golabi P, Younossi Y, et al. Changes in the global burden of chronic liver diseases from 2012 to 2017: the growing impact of NAFLD. Hepatology 2020;72:1605–1616.

[10] **Eslam M**, **Newsome PN**, Sarin SK, et al. A new definition for metabolic dysfunction-associated fatty liver disease: an international expert consensus statement. J Hepatol 2020;73:202–209.
[11] Rinella ME, Lazarus JV, Ratziu V, et al. A multisociety Delphi consensus statement on new fatty liver disease nomenclature. J Hepatol 2023;79:1542–1556.
[12] Tomita K, Teratani T, Suzuki T, et al. p53/p66Shc-mediated signaling contributes to the progression of non-alcoholic steatohepatitis in humans and mice. J Hepatol 2012;57:837–843.
[13] Buitrago-Molina LE, Marhenke S, Longerich T, et al. The degree of liver injury determines the role of p21 in liver regeneration and hepatocarcinogenesis in mice. Hepatology 2013;58:1143–1152.
[14] Torbenson M, Yang SQ, Liu HZ, et al. STAT-3 overexpression and p21 up-regulation accompany impaired regeneration of fatty livers. Am J Pathol 2002;161:155–161.
[15] Aravinthan A, Scarpini C, Tachtatzis P, et al. Hepatocyte senescence predicts progression in non-alcohol-related fatty liver disease. J Hepatol 2013;58:549–556.
[16] Humpton TJ, Hall H, Kiourtis C, et al. p53-mediated redox control promotes liver regeneration and maintains liver function in response to CCl(4). Cell Death Differ 2022;29:514–526.
[17] Zhang X, Zhou D, Strakovsky R, et al. Hepatic cellular senescence pathway genes are induced through histone modifications in a diet-induced obese rat model. Am J Physiol Gastrointest Liver Physiol 2012;302:G558–G564.
[18] **Zheng K**, **Hao F**, **Medrano-Garcia S**, et al. Neuroblastoma RAS viral oncogene homolog (N-RAS) deficiency aggravates liver injury and fibrosis. Cell Death Dis 2023;14:514.
[19] **Graupera I**, **Isus L**, **Coll M**, et al. Molecular characterization of chronic liver disease dynamics: from liver fibrosis to acute-on-chronic liver failure. JHEP Rep 2022;4:100482.
[20] **Garcia Garcia de Paredes A**, **Manicardi N**, **Tellez L**, et al. Molecular profiling of decompensated cirrhosis by a novel microRNA signature. Hepatol Commun 2021;5:309–322.
[21] Benede-Ubieto R, Estevez-Vazquez O, Guo F, et al. An experimental DUAL model of advanced liver damage. Hepatol Commun 2021;5:1051–1068.
[22] Guo F, Zheng K, Benede-Ubieto R, et al. The Lieber-DeCarli diet-a flagship model for experimental alcoholic liver disease. Alcohol Clin Exp Res 2018;42:1828–1840.
[23] Meijnikman AS, Herrema H, Scheithauer TPM, et al. Evaluating causality of cellular senescence in non-alcoholic fatty liver disease. JHEP Rep 2021;3:100301.
[24] Lasry A, Ben-Neriah Y. Senescence-associated inflammatory responses: aging and cancer perspectives. Trends Immunol 2015;36:217–228.
[25] Hotta K, Kitamoto A, Kitamoto T, et al. Identification of differentially methylated region (DMR) networks associated with progression of nonalcoholic fatty liver disease. Sci Rep 2018;8:13567.
[26] Viollet B, Foretz M, Guigas B, et al. Activation of AMP-activated protein kinase in the liver: a new strategy for the management of metabolic hepatic disorders. J Physiol 2006;574:41–53.
[27] King TD, Song L, Jope RS, et al. AMP-activated protein kinase (AMPK) activating agents cause dephosphorylation of Akt and glycogen synthase kinase-3. Biochem Pharmacol 2006;71:1637–1647.
[28] Ramirez T, Li YM, Yin S, et al. Aging aggravates alcoholic liver injury and fibrosis in mice by downregulating sirtuin 1 expression. J Hepatol 2017;66:601–609.
[29] Dzamko N, Schertzer JD, Ryall JG, et al. AMPK-independent pathways regulate skeletal muscle fatty acid oxidation. J Physiol 2008;586:5819–5831.
[30] Abdul-Wahed A, Guilmeau S, Postic C. Sweet sixteenth for ChREBP: established roles and future goals. Cell Metab 2017;26:324–341.
[31] National Institute of diabetes and digestive and kidney diseases. Palbociclib. LiverTox: clinical and research information on drug-induced liver injury. Bethesda (MD): NIDDKD; 2012. Available from: https://www.ncbi.nlm.nih.gov/books/NBK547882/.
[32] Bollard J, Miguela V, Ruiz de Galarreta M, et al. Palbociclib (PD-0332991), a selective CDK4/6 inhibitor, restricts tumour growth in preclinical models of hepatocellular carcinoma. Gut 2017;66:1286–1296.
[33] Younossi Z, Tacke F, Arrese M, et al. Global perspectives on nonalcoholic fatty liver disease and nonalcoholic steatohepatitis. Hepatology 2019;69:2672–2682.
[34] Bonnet L, Alexandersson I, Baboota RK, et al. Cellular senescence in hepatocytes contributes to metabolic disturbances in NASH. Front Endocrinol (Lausanne) 2022;13:957616.
[35] Shiraki K, Wagayama H, Asada M, et al. Cytoplasmic p21(WAF1/CIP1) expression in human hepatocellular carcinomas. Liver Int 2006;26:1018–1019.
[36] Wagayama H, Shiraki K, Sugimoto K, et al. High expression of p21WAF1/CIP1 is correlated with human hepatocellular carcinoma in patients with hepatitis C virus-associated chronic liver diseases. Hum Pathol 2002;33:429–434.
[37] Aravinthan A, Pietrosi G, Hoare M, et al. Hepatocyte expression of the senescence marker p21 is linked to fibrosis and an adverse liver-related outcome in alcohol-related liver disease. PLoS One 2013;8:e72904.
[38] Ogrodnik M, Miwa S, Tchkonia T, et al. Cellular senescence drives age-dependent hepatic steatosis. Nat Commun 2017;8:15691.
[39] Ehedego H, Boekschoten MV, Hu W, et al. p21 ablation in liver enhances DNA damage, cholestasis, and carcinogenesis. Cancer Res 2015;75:1144–1155.
[40] Karimian A, Ahmadi Y, Yousefi B, et al. Multiple functions of p21 in cell cycle, apoptosis and transcriptional regulation after DNA damage. DNA Repair (Amst) 2016;42:63–71.
[41] Childs BG, Gluscevic M, Baker DJ, et al. Senescent cells: an emerging target for diseases of ageing. Nat Rev Drug Discov 2017;16:718–735.
[42] Wang JW, Wan XY, Zhu HT, et al. Lipotoxic effect of p21 on free fatty acid-induced steatosis in L02 cells. PLoS One 2014;9:e96124.
[43] Zhao Y, Hu X, Liu Y, et al. ROS signaling under metabolic stress: cross-talk between AMPK and AKT pathway. Mol Cancer 2017;16:79.
[44] Foster DW. Malonyl-CoA: the regulator of fatty acid synthesis and oxidation. J Clin Invest 2012;122:1958–1959.
[45] Liu J, Huang K, Cai GY, et al. Receptor for advanced glycation end-products promotes premature senescence of proximal tubular epithelial cells via activation of endoplasmic reticulum stress-dependent p21 signaling. Cell Signal 2014;26:110–121.
[46] Lee JY, Bielawska AE, Obeid LM, et al. Regulation of cyclin-dependent kinase 2 activity by ceramide. Exp Cell Res 2000;261:303–311.
[47] Wiley CD, Velarde MC, Lecot P, et al. Mitochondrial dysfunction induces senescence with a distinct secretory phenotype. Cell Metab 2016;23:303–314.
[48] Attia MF, Ogunnaike EA, Pitz M, et al. Enhancing drug delivery with supramolecular amphiphilic macrocycle nanoparticles: selective targeting of CDK4/6 inhibitor palbociclib to melanoma. Biomater Sci 2024;12:725–737.
[49] Finn RS, Crown JP, Lang I, et al. The cyclin-dependent kinase 4/6 inhibitor palbociclib in combination with letrozole versus letrozole alone as first-line treatment of oestrogen receptor-positive, HER2-negative, advanced breast cancer (PALOMA-1/TRIO-18): a randomised phase 2 study. Lancet Oncol 2015;16:25–35.
[50] Turner NC, Ro J, Andre F, et al. Palbociclib in hormone-receptor-positive advanced breast cancer. N Engl J Med 2015;373:209–219.

Keywords: CDKN1A; Steatotic liver disease (SLD); Hepatocyte; Senescence; Metabolic dysregulation; Palbociclib.
Received 19 March 2024; received in revised form 14 September 2024; accepted 1 October 2024; Available online 5 October 2024